Activity 10: Ambient air quality monitoring

Activity 10.3: E-bam deployment and air quality assessment for KwaZamokuhle for 2023 (during implementation)

Document by:

ARM
AIR RESOURCE MANAGEMENT

Final Report

10th July 2024

Document Title

Client		**Eskom**
Title		**E-bam deployment and air quality assessment for Kwazamokuhle for 2023 (during implementation)**
Our Reference		**ESKPMV-2023- ACT-10.3-00**
Issued to Client		**10th July 2024**
Classification		**Company Confidential**

Document Change Record

Revision Number	Date	Description of Revision
00A	18th May 2024	Creation of Document
00B	6th June 2024	Peer Review of Document
00	13th June 2024	Draft Document issued to Eskom
01	10th July 2024	Final Document issued to Eskom

Document Approval

	Name	Date
Prepared by	Avishkar Ramandh & Anesu Shamu	9th July 2024
Reviewed by	Fred Goede	10th July 2024
Approved by	Fred Goede	10th July 2024

TABLE OF CONTENTS

TABLE OF FIGURES

EXECUTIVE SUMMARY

STUDY OBJECTIVE

The objective of this study component was to conduct ambient air quality monitoring utilising the Environmental Beta Attenuation Monitors (E-BAM) to measure baseline particulate matter (PM_{10} and $Pm_{2.5}$) ambient concentrations in Kwazamokuhle. The study performed an analysis of the particulate matter ambient air quality baseline trends, correlations and general relations. It's noted that these measurements at KwaZamokuhle were conducted during the active rollout of the Eskom AQO Project interventions in the KwaZamokuhle community and thus serves as the status quo air quality baseline herein.

2. STUDY METHODOLOGY

Five E-BAM Environmental Beta Attenuation Mass Monitors were commissioned at five residential sampling sites (three PM_{10} and two $PM_{2.5}$ measurements) in the KwaZamokuhle region. The E-BAM instrument is a portable, real-time beta gauge comparable to U.S.-EPA methods for $PM_{2.5}$ and PM_{10} particulate measurements. The E-BAM automates particulate measurement by continuously sampling and reporting concentration data. The sampling assessment was conducted from mid-May to mid-September 2023 at the five residential sampling sites. Additionally, an analysis is provided for both sulfur dioxide (SO_2) and nitrogen dioxide (NO_2) pollutant concentrations which was obtained from the Eskom KwaZamokuhle air quality monitoring station (AQMS) which is located at KwaZamokuhle. The Openair model was utilised to statistically analyse the semi-empirical mathematical relationships between air pollutant concentrations and meteorological parameters for these five sites.

3. STUDY RESULTS

The following section presents the study findings for: particulate matter ($PM_{2.5}$ and PM_{10}); sulfur dioxide (SO_2) and nitrogen dioxide (NO_2).

3.1 PARTICULATE MATTER (PM_{10} & $PM_{2.5}$)

As illustrated by Figure i, the daily NAAQS for PM_{10} of 75 µg/m3 is exceeded at all four sampling locations, especially during the colder months of May to September, which indicate higher daily ambient concentrations.

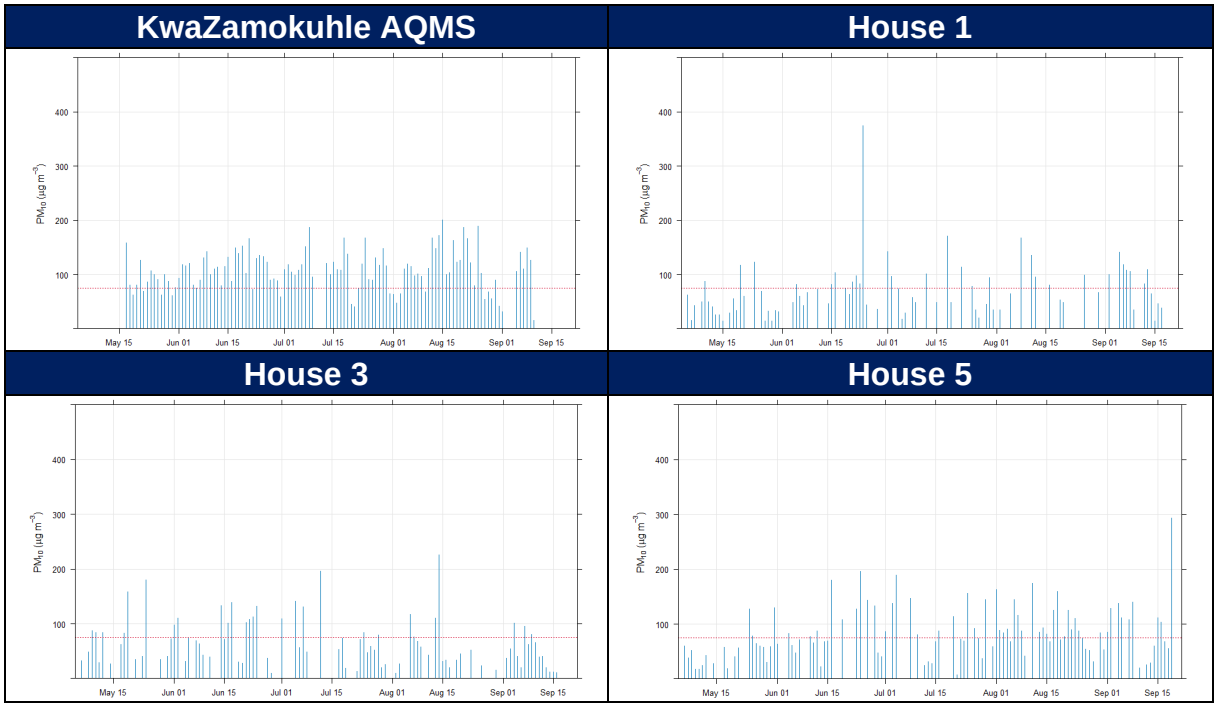

Figure i: Daily ambient PM_{10} concentrations (µg/m^3) measured at the sampling sites during the sampling survey

Similarly Figure ii illustrates the daily NAAQS for $PM_{2.5}$ of 40 µg/m^3 is exceeded multiple times at both sampling sites. It's noted that maximum daily $PM_{2.5}$ concentrations of around 150 µg/m was recorded at these houses.

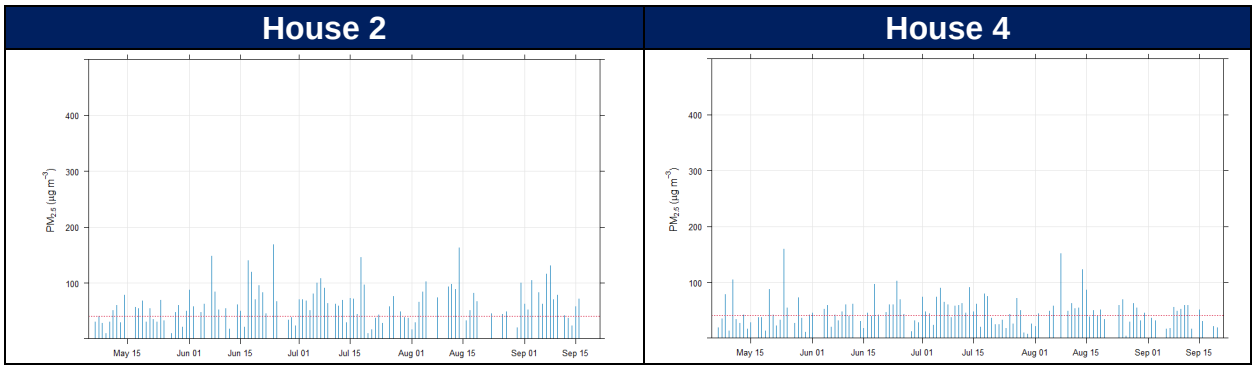

Figure ii: Daily ambient PM_{10} concentrations ($\mu g/m^3$) measured at the sampling sites during the sampling survey

The Openair analysis indicated that a morning peak occurs between 06:00 and 07:00 whilst the evening peak between18:00 and 19:00. This bi-modal particulate matter peak is a typical profile for residential fuel burning. The morning peaks reduces towards midday as the inversion layer rises & improves the mixing height of the planetary boundary layer.

Its noteworthy that at all sampling locations, there is an increase in elevated particulate matter concentrations for the winter months of June, July and August whilst a notable decrease is observed for September. The colder ambient temperatures in winter lead to an increase in residential fuel burning activities. Fewer instances of particulate matter exceeding limits were observed in the warmer month of September due to reduced space heating requirements.

3.2 SULPHUR DIOXIDE (SO_2)

An examination of the Eskom KwaZamokuhle AQMS revealed only one exceedance of the hourly NAAQS SO_2 standard. No exceedances of the daily NAAQS for SO_2 were recorded for the stations during the sampling period. A consistent SO_2 peak was evident throughout the entire week at 18:00 in the winter months. The Openair analysis supported that the detected 18:00 peak was a result of residential fuel burning emissions.

3.3 NITROGEN DIOXIDE (NO_2)

A review of the Eskom KwaZamokuhle AQMS indicated no instances of surpassing the hourly NAAQS NO2 standard. The peak average concentrations were observed between 06:00 to 08:00 and 17:00 to 19:00 at the Eskom KwaZamokuhle AQMS. The Openair analysis specifically identified vehicle emissions as the primary factor influencing the variability of NO2 concentrations. The daily pattern aligns with the traffic volume fluctuations, showing pronounced peaks in concentration during weekday rush hours in the early morning and late afternoon.

4. CONCLUSION

The 2023 survey campaign has illustrated that increased short-term levels of particulate matter during winter months are directly linked to residential fuel burning in Kwazamokuhle. The daily NAAQS for particulate matter. The Openair analysis further confirmed that the elevated concentrations of particulate matter observed in winter were linked to localized non-buoyant sources (residential fuel burning) rather than emissions from tall stacks. The survey campaign clearly indicates that residential fuel burning poses a significant health hazard to the Kwazamokuhle community. Therefore, there is an opportunity to decrease human exposure to harmful air pollution levels by reducing emissions from residential burning, thereby supporting the implementation of Eskom's PMV air quality offset intervention project in Kwazamokuhle.

1. BACKGROUND

1.1 Air Quality Offsets Guideline

An environmental offset is an action(s), designed to compensate for a negative environmental impact of resource use, a discharge, emission or other activity. The Department of Forestry, Fisheries and the Environment (DFFE) defines air emissions offsets as an intervention, or interventions, specifically implemented to counterbalance the adverse and residual environmental impact of atmospheric emissions in order to deliver a net ambient air quality benefit within, but not limited to, the affected airshed where ambient air quality standards are being or have the potential to be exceeded and whereby opportunities and need for offsetting exist (Notice 333 of 2016).

1.2 ESKOM'S Approach to Air Quality Offsets

DFFE's Air Quality Offset Guideline has shaped and informed Eskom's Air Quality Offsets Implementation Plan. This Plan has been based on a scientific process of feasibility studies, testing and demonstration, and on consultation with key stakeholders. Figure 1 illustrates the concept schedule for the phased implementation of Eskom's air quality offsets.

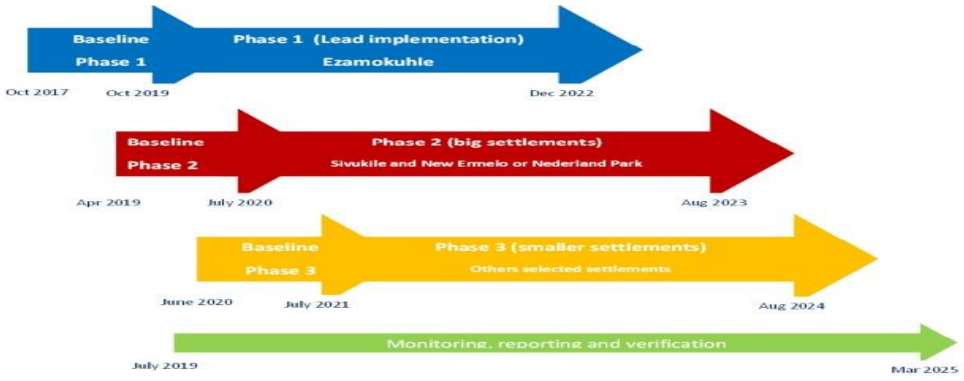

Figure 1: Concept Schedule for the implementation of Eskom's air quality offsets (Matimolane, 2020).

Eskom has adopted the phased approach (Figure 2) herein to increase the probability of success and to ensure that learnings from early phases are incorporated into the large-scale roll-out. (Matimolane, 2020).

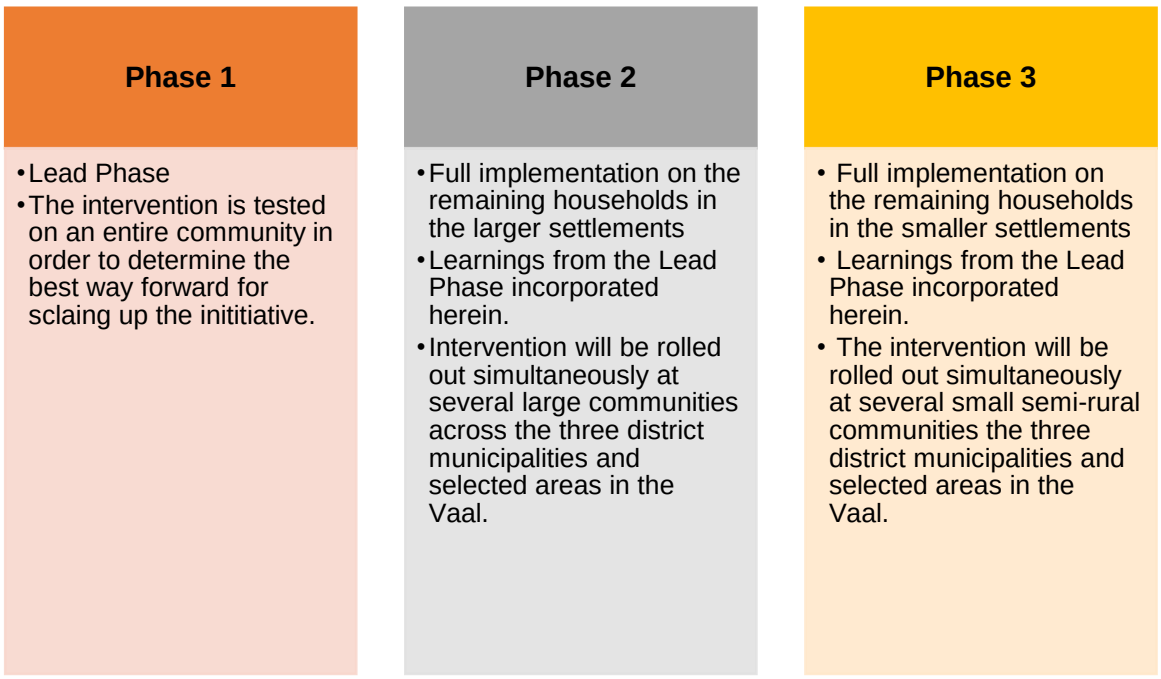

Figure 2: Eskom's Phased approach to the rollout of air quality offset interventions (Matimolane, 2020).

Eskom's air quality offsets programme is designed to reduce human exposure to harmful levels of air pollution by reducing emissions from local sources, like domestic coal burning and waste burning. Thus, air quality offsets can improve ambient air quality in low-income communities in the vicinity of Eskom's power stations. Eskom has developed air quality offset (AQO) implementation plans for Majuba Power Station (eZamokuhle township); Hendrina Power Station (KwaZamokuhle township) and Lethabo Power station (Sharpeville).

1.3 ESKOM'S PLANNING, MONITORING AND VERIFICATION (PMV) PROJECT

For Eskom's PMV Project, interventions to reduce household emissions from domestic coal/wood burning will be rolled out in KwaZamokuhle and eZamokuhle in the Mpumalanga Highveld. For formal dwellings the intervention will be a thermal insulation retrofit and an electricity starter pack and installation. The intervention for informal dwellings still needs to be selected and tested. Interventions also need to be identified and implemented to improve air quality in Sharpeville, Gauteng. Since domestic coal burning is less prevalent in Sharpeville, it is expected that a community-scale intervention, like reducing waste burning, will be more suitable there.

Air Resource Management (ARM) (Pty) Ltd has been appointed by Eskom to support the PMV services in support of the *Phase 1: Lead implementation* at: KwaZamokuhle; eZamokuhle and Sharpeville. Its ARM (Pty) Ltd understanding that the overall objective *Lead Implementation Phase* is to benefit the specific local communities, minimize implementation risk, increase practical and scientific knowledge, and develop and refine monitoring, reporting and verifications processes. To achieve this, Eskom has included sixteen targeted work package Activities (Table 1) for these respective communities. This report focuses on *Activity 10.3: E-bam deployment and air quality assessment for Kwazamokuhle for 2023 (during implementation)*

Table 1: Eskom PMV Activity Schedule (Eskom PMV NEC Contract)

Activities	Kwazamokuhle	Ezamokuhle	Sharpeville
Activity 1: Preliminary air quality assessment		✓	
Activity 2: Gather Area intelligence		✓	
Activity 3: Rapid in situ assessment		✓	
Activity 4: Obtain ethical clearance		✓	
Activity 5: Census	✓	✓	✓
Activity 6: Community source survey		✓	
Activity 7: Fuel source survey		✓	
Activity 8: Household surveys		✓	
Activity 9: Annual (household/community) surveys and monitoring of project effectiveness	✓	✓	✓
Activity 10: Ambient air quality monitoring	✓	✓	✓
Activity 11: Conduct indoor air quality monitoring	✓	✓	
Activity 12: Atmospheric Dispersion Model	✓	✓	✓
Activity 13: Design of Intervention		✓	✓
Activity 14: Development of Database Reporting	✓	✓	✓
Activity 15: Strategic Assistance and offsets methodology	✓	✓	✓
Activity 16: Research and Development	✓	✓	✓

1.4 Scope of Work

In accordance with the scope of work, for Activity 10: *Conduct Ambient Air Quality Monitoring*, ARM is to conduct ambient air quality monitoring utilising the Environmental beta Attenuation Monitors to monitor baseline PM concentrations in Kwazamokuhle before the implementation and rollout of the intended Eskom household interventions.

2. METHODOLOGY

2.1 SAMPLING METHODOLOGY

Five E-BAM Environmental Beta Attenuation Mass Monitors were commissioned at five residential sampling sites in the KwaZamokuhle region. The E-BAM instrument is a portable, real-time beta gauge comparable to U.S.-EPA methods for $PM_{2.5}$ and PM_{10} particulate measurements. The E-BAM automates particulate measurement by continuously sampling and reporting concentration data. Data records are updated every minute. Figure 3 is a graphical representation of the E-BAM instrument.

Figure 3: E-Bam Instrument

2.2 SAMPLING LOCATIONS

Table 2 is a summary of the E-BAM sampling locations as well as the sampling duration. Figure 4 is a picture of the E-BAM instrument commissioned at Houses 2 and 5 whereas Figure 5 is a close-up of these sampling locations in the KwaZamokuhle residential region.

Figure 6 is locality map of the E-BAM samplers in relation to the Eskom Komati and Eskom Hendrina power stations, whilst Figure 7 is indicative of the KwaZamokuhle residential region in the Highveld.

Table 2: Summary of E-BAM sampling locations

Site	Pollutant Measured	Latitude (°S)	Longitude (°E)	Sampling Duration
House 1	PM_{10}	-26.131308	29.730162	5th May 2023 - 21 September 2023
House 2	$PM_{2.5}$	-26.133685	29.734096	6th May 2023 - 21 September 2023
House 3	PM_{10}	-26.128971	29.737095	6th May 2023 - 21 September 2023
House 4	$PM_{2.5}$	-26.136925	29.727320	6th May 2023 - 21 September 2023
House 5	PM_{10}	-26.147458	29.730104	6th May 2023 - 21 September 2023

Figure 4: E-Bam instrument commissioned at House 2 (left) and House 5 (right).

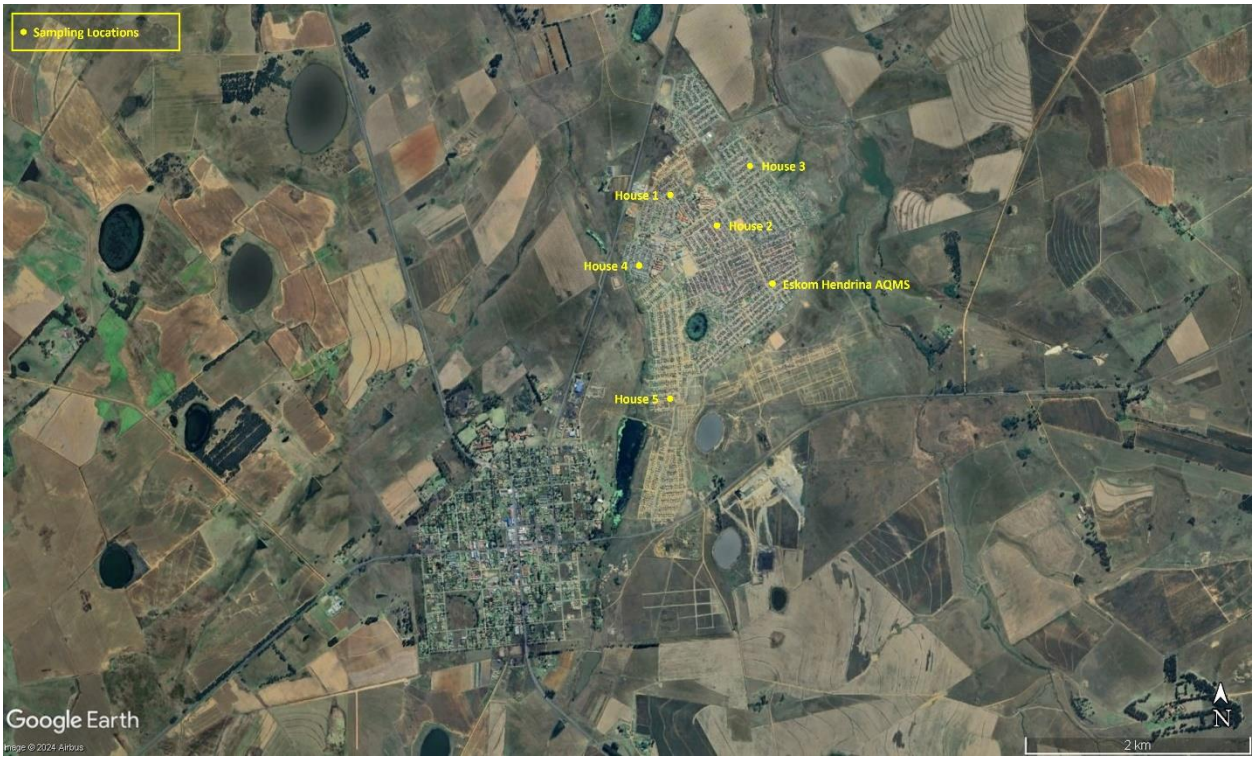

Figure 5: Close-up of the sampling sites in the KwaZamokuhle community.

Figure 6: Map indicating the sampling sites in relation to the Hendrina and Komati Power Stations.

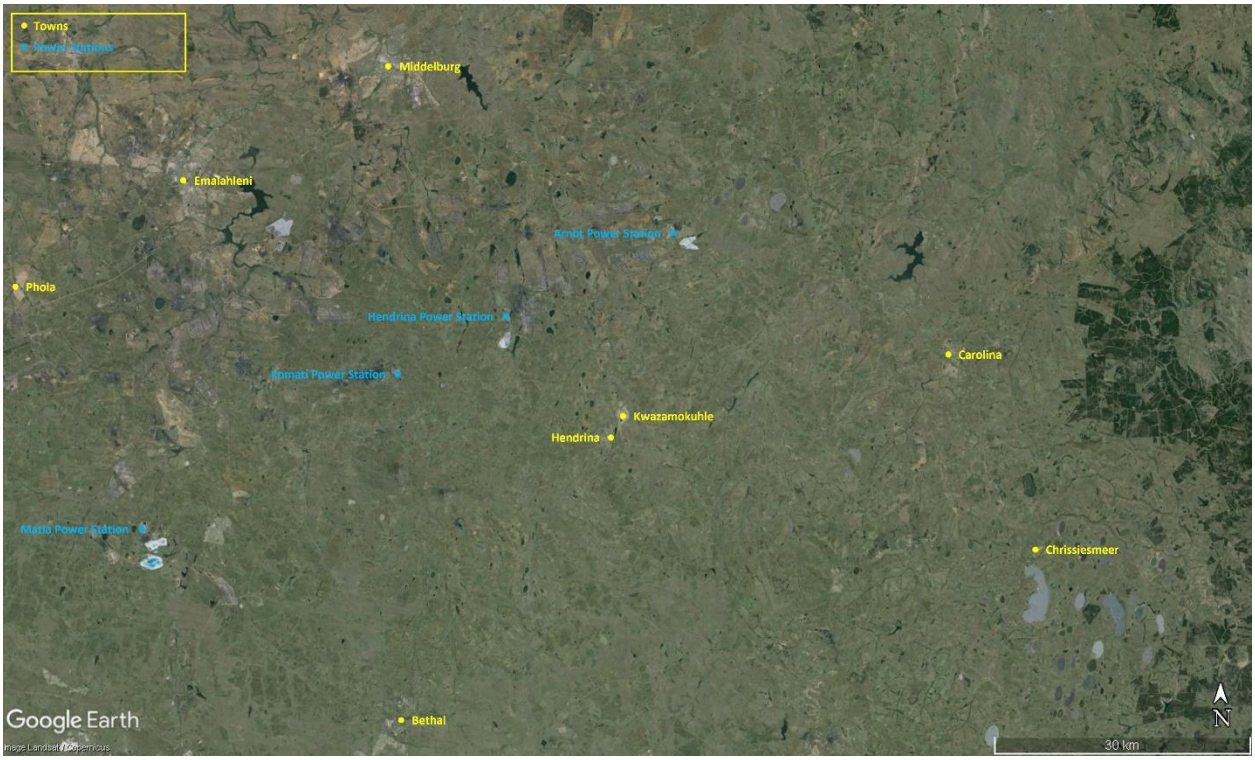

Figure 7: Layout of KwaZamokuhle in the greater Highveld region.

3. RESULTS AND DISCUSSION

3.1 METEOROLOGICAL RESULTS

Air quality is strongly influenced by meteorology. Meteorological mechanisms govern the dispersion and eventual removal of pollutants from the atmosphere (Seaman, 2000). The analysis of hourly average meteorological data is necessary to facilitate a comprehensive understanding of the dispersion potential of the site. The horizontal dispersion of pollution is largely a function of the wind field. The wind speed determines both the distance of downward transport and the rate of dilution of pollutants. The wind rose is a useful indication for indicating how wind speed and wind direction conditions vary by year. Meteorological data for the sampling period were obtained from the Eskom KwaZamokuhle AQMS.

3.1.1 WIND SPEED AND WIND DIRECTION

Wind drives the atmospheric transport and strongly affects vertical air mixing and thus the ventilation of the urban air (Grundstrom et al., 2015). The understanding of how wind speed affects ground–level air pollution concentrations is relatively well established.

Stagnant atmospheric conditions with calm, clear weather often led to stable atmospheric stratification which can transform into strong nocturnal temperature inversions due to rapid surface cooling. The resulting restriction in vertical air mixing near the surface consequently leads to poor air quality (Delaney and Dowding, 1998; Janhall et. al., 2006; Olofson et al., 2009). Low wind speeds deteriorate air quality with respect to pollutants emitted near the ground due to restricted air ventilation (Jones et al., 2010). In contrast higher wind speeds are associated with increased dispersion and mixing of atmospheric pollutants which may result in low ambient pollution concentrations. Figure 8 illustrates

the predominant wind directions for the sampling period for the Eskom KwaZamokuhle AQMS.

For the Eskom KwaZamokuhle AQMS station the average wind speed for the sampling period (Figure 8) was recorded at 2.51m/s with calm condition 0.4%. Calm condition means that wind speed is recorded at zero meter/second (Carlaw, 2015). The predominant wind direction was north westerly (≈24% frequency of occurrence) followed by southerly winds (≈17% frequency of occurrence) with maximum wind speed of 11 – 17m/s.

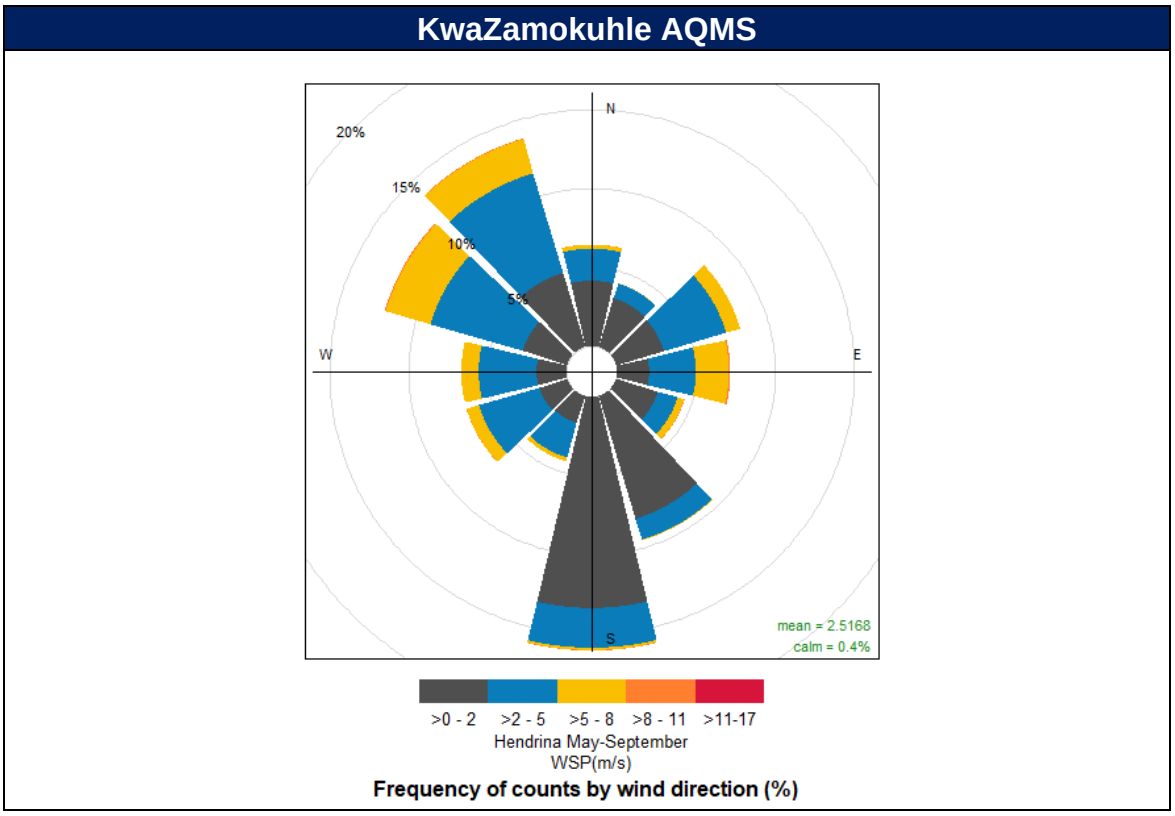

Figure 8: Wind roses for the Eskom KwaZamokuhle AQMS for the sampling period

Figure 9 provides the diurnal wind speed, whilst Figure 10 is indicative of the monthly mean ambient wind speeds recorded at the Eskom KwaZamokuhle AQMS.

It is evident from Figure 9 that the wind speed for both stations increase at 08:00 with a decrease at around 17:00. Maximum wind speeds are recorded at 13:00. Figure 10 illustrates slightly higher monthly mean wind speeds during September for the KwaZamokuhle AQMS. The box plots highlight the distribution of the wind speed values by showing the minimum values, lower quartile, median, upper quartile and maximum values, and outlier values (circles outside of the box area depicted on the y-axis).

As a norm, wind speeds in excess of 5.4m/s potentially have sufficient energy to pick-up and transport loose and/or disturbed particulate matter, which gives rise to visible nuisance dust and clouds of dust at ground level. The extent, to which this occurs / can occur, depends on several parameters, such as the properties and characteristics of the particulate matter, moisture content, etc.

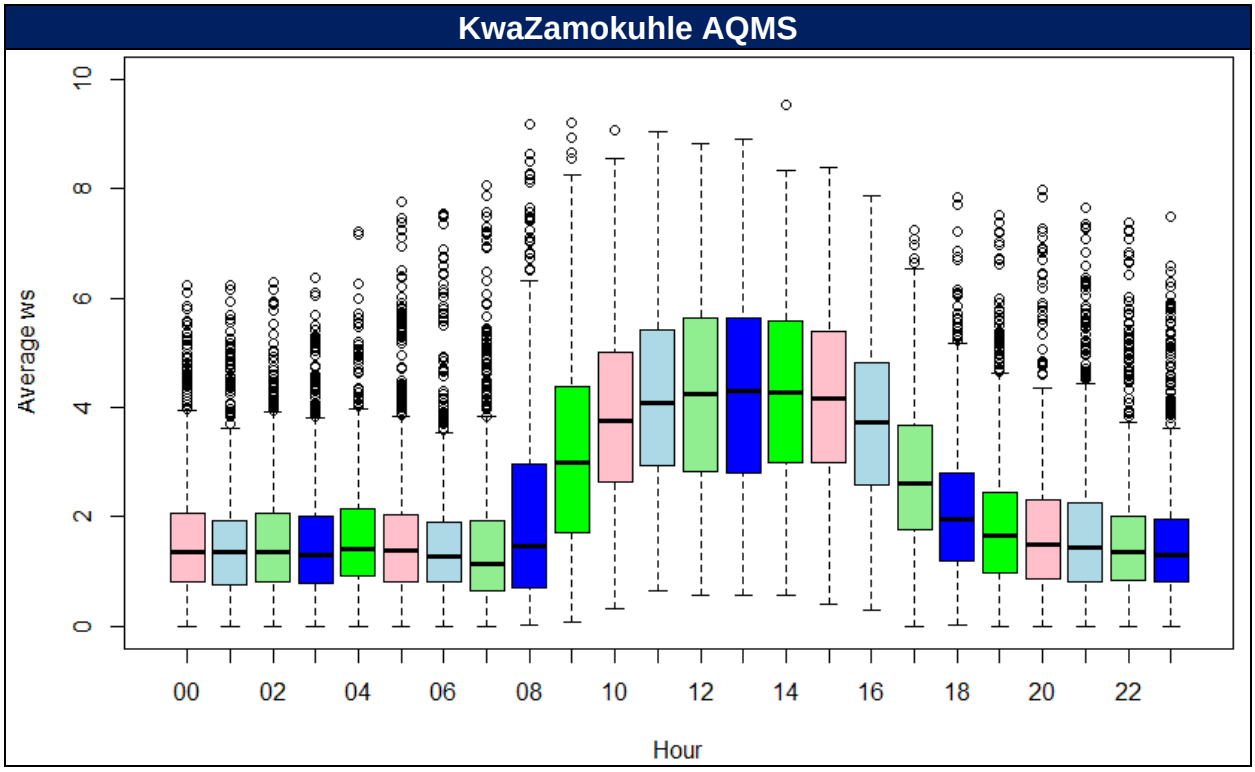

Figure 9: Diurnal wind speeds recorded at the KwaZamokuhle AQMS (m/s).

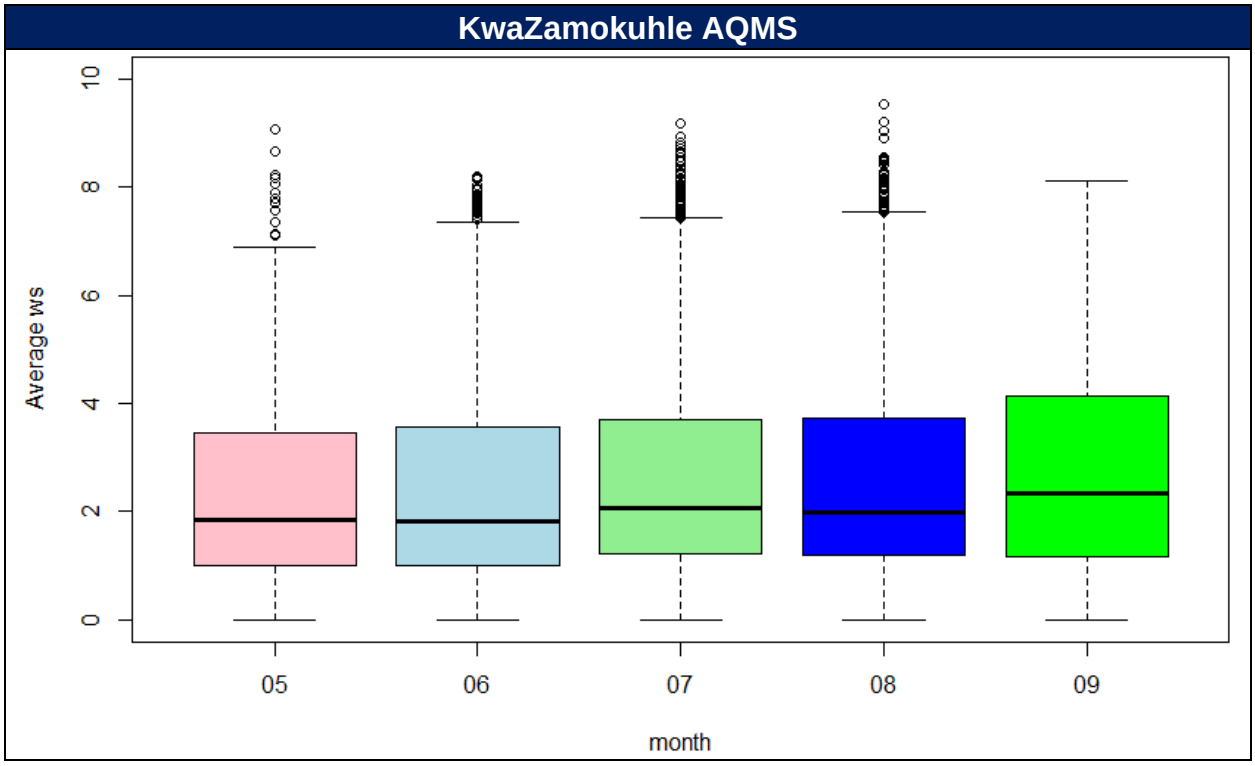

Figure 10: Monthly mean wind speeds recorded at the KwaZamokuhle AQMS (m/s).

3.1.2 TEMPERATURE

Air temperature is important, both for determining the effect of plume buoyancy (the larger the temperature difference between the plume and the ambient air, the higher the plume can rise), and determines the development of the mixing and inversion layers. Figure 11 provides daily mean ambient temperatures for the Eskom KwaZamokuhle AQMS. From Figure 11, it is evident how the average ambient air temperatures are between 8 and 17°C for May, slowly increasing to 4 and 11°C for the month of July September indicate an increase to 20°C. An increase in wind speed and ambient temperature improves the dispersion of air pollutants in the air.

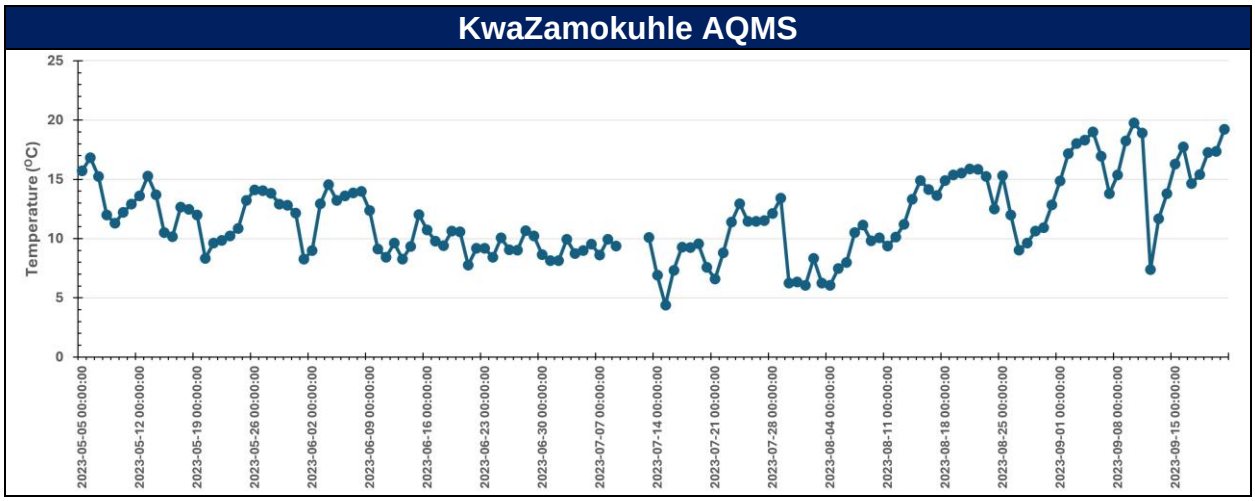

Figure 11: Daily average temperature at the KwaZamokuhle AQMS (°C).

3.1.3 RAINFALL

Figure 12 provides daily total rainfall/precipitation recorded for the Eskom KwaZamokuhle AQMS. From Figure 12, it is evident both stations recorded a maximum rainfall of 0.23mm on 7 May 2023. Frequent rainfall events were recorded during May 2023. Overall, little precipitation was recorded at the KwaZamokuhle AQMS during the sampling period.

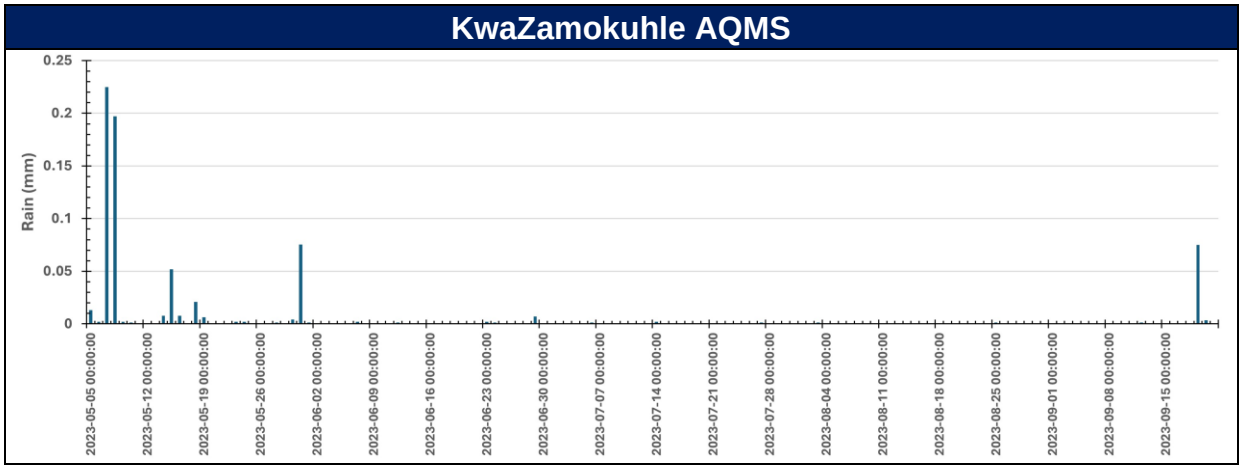

Figure 12: Daily total precipitation (rainfall) at the KwaZamokuhle AQMS (mm).

3.2 POLLUTANT TREND & ANALYSIS

Openair is an air quality model for statistically analysing semi-empirical mathematical relationships between air pollutant concentration and other factors that may affect it (Tiwary, 2010). The Openair model can analyse emissions of pollutant sources, pollutant characteristics, trend estimates and model evaluations. Additionally, Openair model has the advantage of data manipulation or interpolation, statistical data analysis, creation, and visualization of high-quality graphics (Carslaw, 2015).

The Openair model has been successfully applied to determine the potential emission sources based on urban air quality measurements (Munir et al., 2016, Czernecki et al., 2016) as well as for air quality research campaigns (Crilley et al. 2017), studies concerning pollution exposure (Pattinson et al. 2016), and natural events (Salvador et al. 2014; Schweizer, Cisneros 2014). Often multiple functions provided in Openair are combined to provide comprehensive information & insight for the analysed data (Crilley et al., 2015 and Jang et al., 2016).

The relationship and trends of concentrations, including PM_{10}, $PM_{2.5}$, SO_2, NO_2 and meteorological parameters such as wind speed and direction, temperature for the five sampling sites were examined using the Openair model.

3.2.1 PARTICULATE MATTER (PM_{10})

Figure 13 indicate the ambient hourly PM_{10} concentrations recorded at the Eskom KwaZamokuhle AQMS, House 1, House 3 and House 5 sampling sites. Although no NAAQS exists for hourly PM_{10} concentrations, Figure 13 highlight that for the KwaZamokuhle AQMS maximum hourly concentrations of 500 $\mu g/m^3$ were recorded, whilst Houses 1, 3 and 5 indicate maximum concentrations of 600 to 700 $\mu g/m^3$ respectively. Figure 14 is a graphical representation of the average hourly PM_{10}

concentrations for the sampling period. It is evident from Figure 14 that the highest average values are recorded during hours 06:00 to 08:00 for both the KwaZamokuhle AQMS, House 3 and House 5 sites, but all four sites indicate elevated hourly values from 17:00 to 19:00. These diurnal profiles are also illustrated in Figure 15. The bi-modal particulate matter peak for all four sites (Figure 15) is a typical profile for residential fuel burning. A morning peak occurs between 06:00 and 07:00 whilst the evening peak occurs between 18:00 and 19:00. The morning peaks reduces towards midday as the inversion layer rises & improves the mixing height of the planetary boundary layer.

Figure 16 indicate the daily ambient PM_{10} concentrations recorded at the Eskom KwaZamokuhle AQMS, House 1, House 3 and House 5 sampling sites. The daily NAAQS for PM_{10} of 75 $\mu g/m^3$ is exceeded at all four sampling locations, especially during the colder months of May to September, which indicate higher daily ambient concentrations (Figure 16). Daily maximum PM_{10} concentrations of 200 $\mu g/m^3$ were recorded for both the Eskom KwaZamokuhle AQMS and House 3 sampling sites, whilst House 1 and House 5 recorded maximum concentrations of approximately 400 and 300 $\mu g/m^3$ respectively. These elevated daily concentrations during the colder months are indicated in the calendar plots (Figure 17). These elevated concentrations could be attributed to colder ambient temperatures leading to an increase in residential fuel burning. Figure 18 highlights the average weekday PM_{10} concentrations. The Eskom KwaZamokuhle AQMS indicate a relative concentration of 100 $\mu g/m^3$ for the days of the week, whilst Houses 1 and 5 indicate elevated concentrations for Tuesdays and Saturdays. House 4 indicate elevated concentrations on a Friday.

Figure 19 illustrates the monthly mean ambient PM_{10} concentrations recorded at the sampling locations. All sampling locations indicate an increase in monthly concentrations for June, July and August, whilst a notable decrease is observed for September.

As mentioned previously, the bi-modal particulate matter peak for both the Eskom eZamokuhle, Majuba and House 4 sites (Figure 15) is a typical profile for residential fuel burning. These peaks are evident in Figure 20 illustrating the weekly diurnal ambient PM_{10} concentrations. A morning peak occurs between 06:00 and 07:00 whilst the evening peak occurs between 18:00 and 19:00.

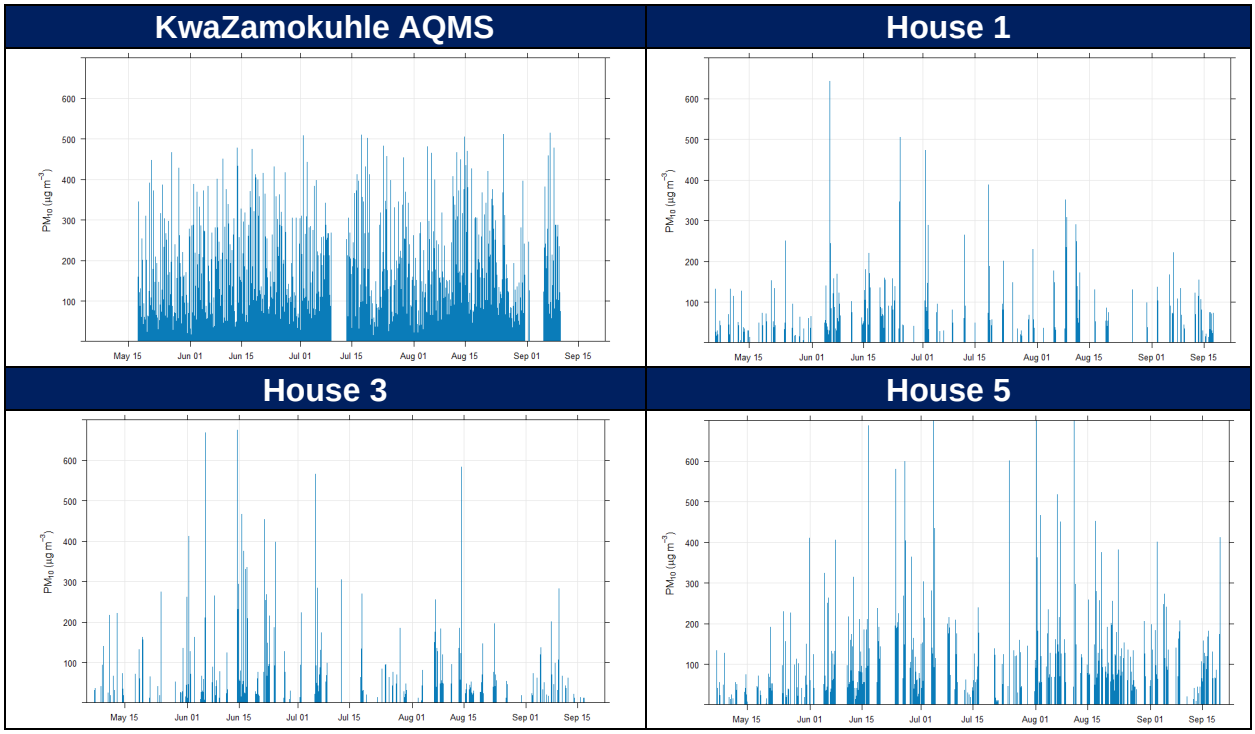

Figure 13: Hourly ambient PM_{10} concentrations (µg/m^3) measured at the sampling locations during the sampling survey.

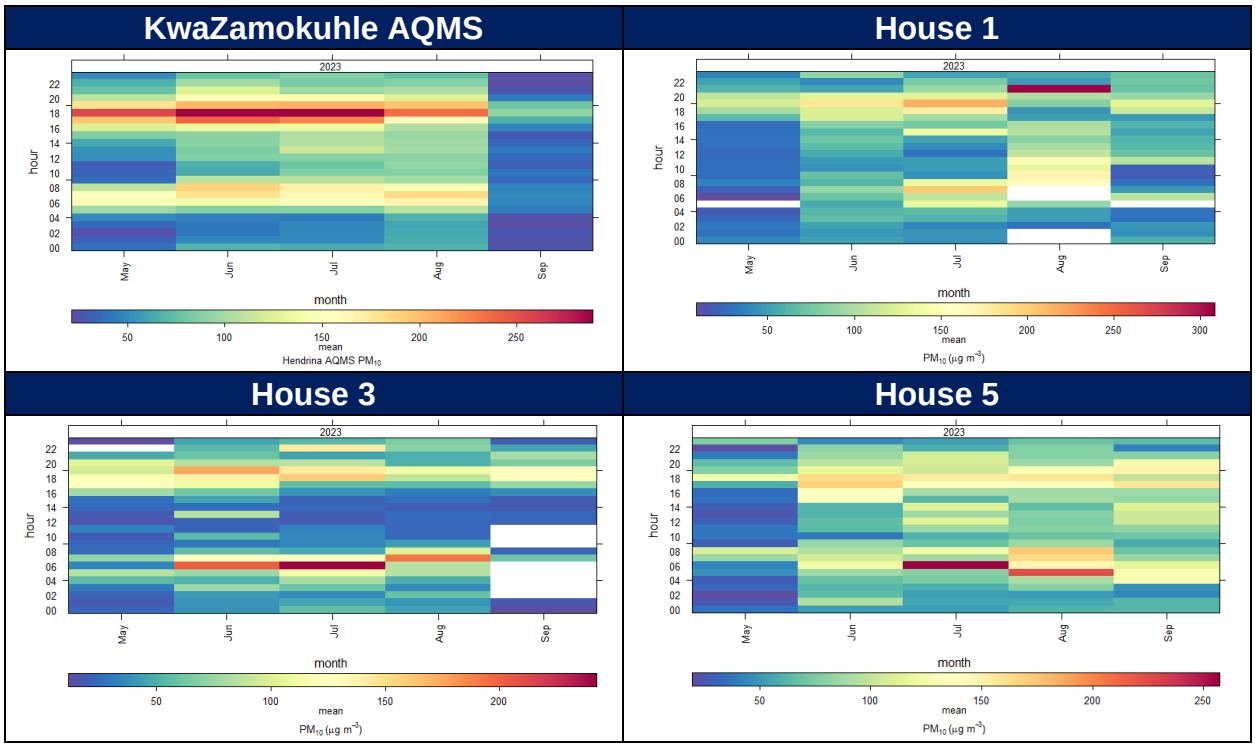

Figure 14: Mean hourly ambient PM_{10} concentrations (µg/m³) measured at the sampling locations during the sampling survey.

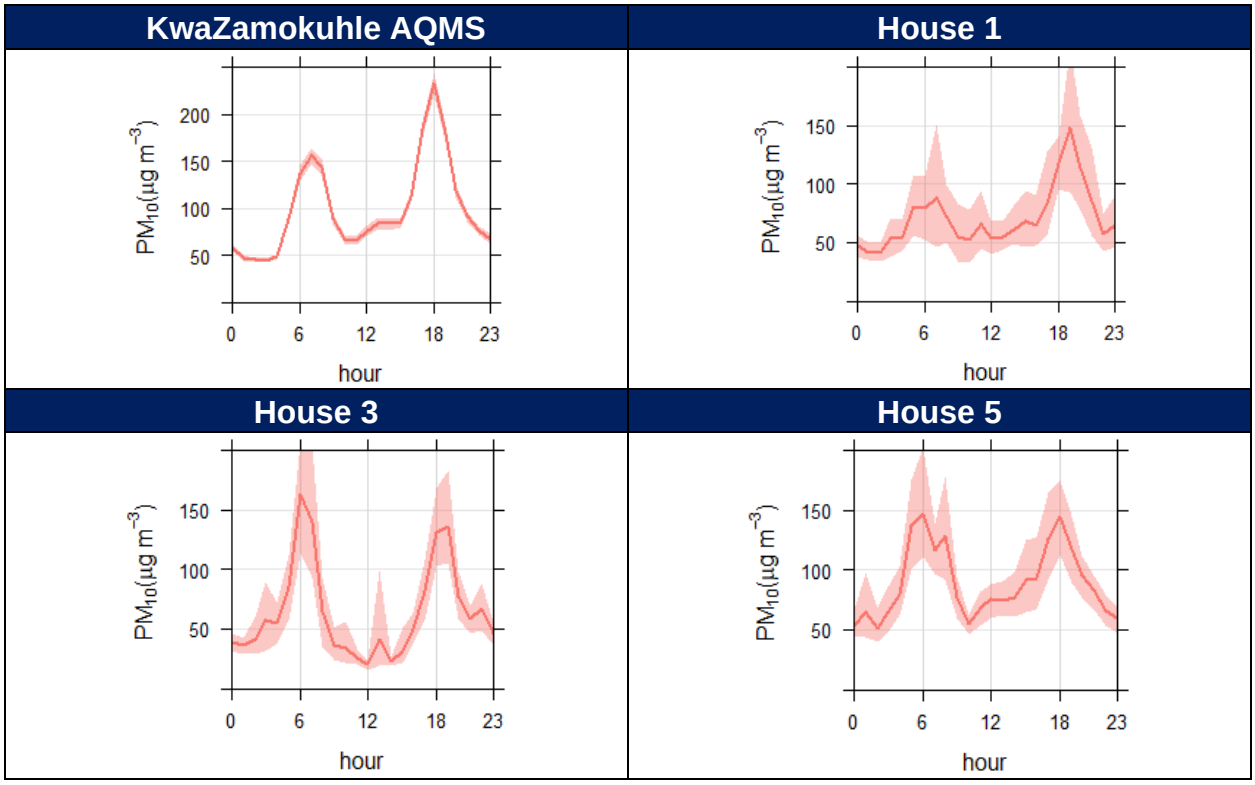

Figure 15: Mean hourly diurnal PM_{10} concentrations (µg/m³) measured at the sampling sites during the sampling survey.

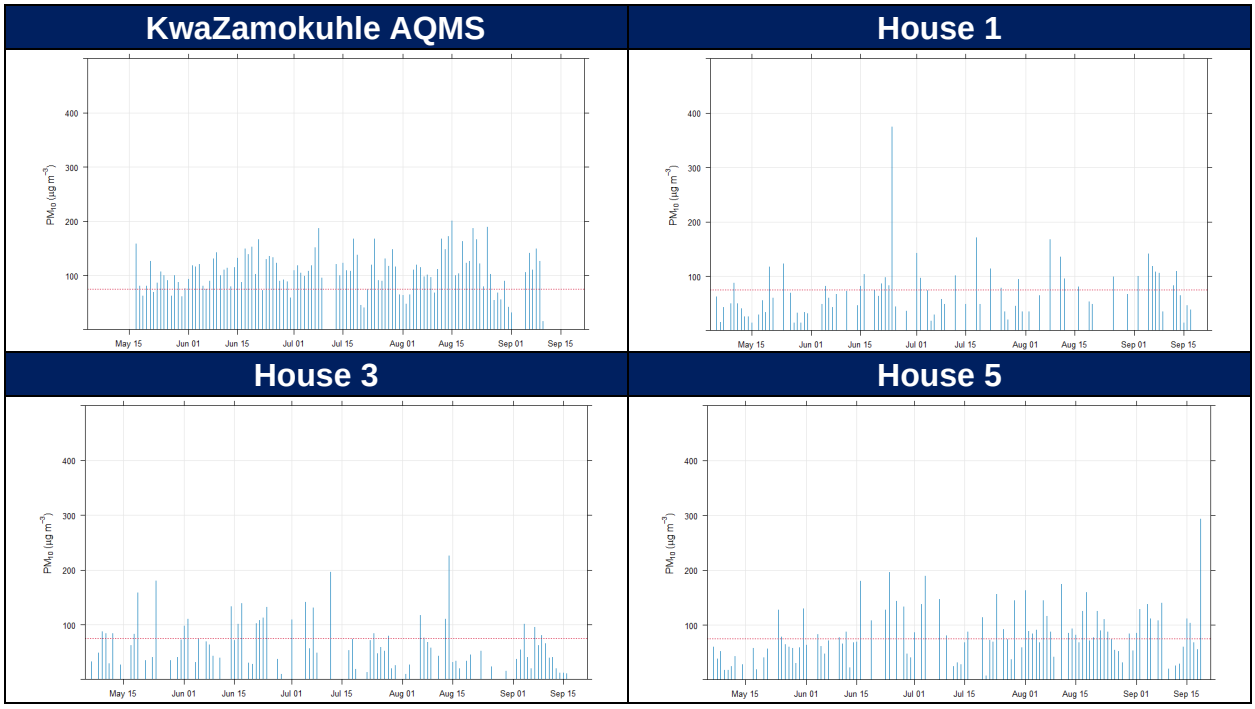

Figure 16: Daily ambient PM_{10} concentrations (µg/m^3) measured at the sampling sites during the sampling survey.

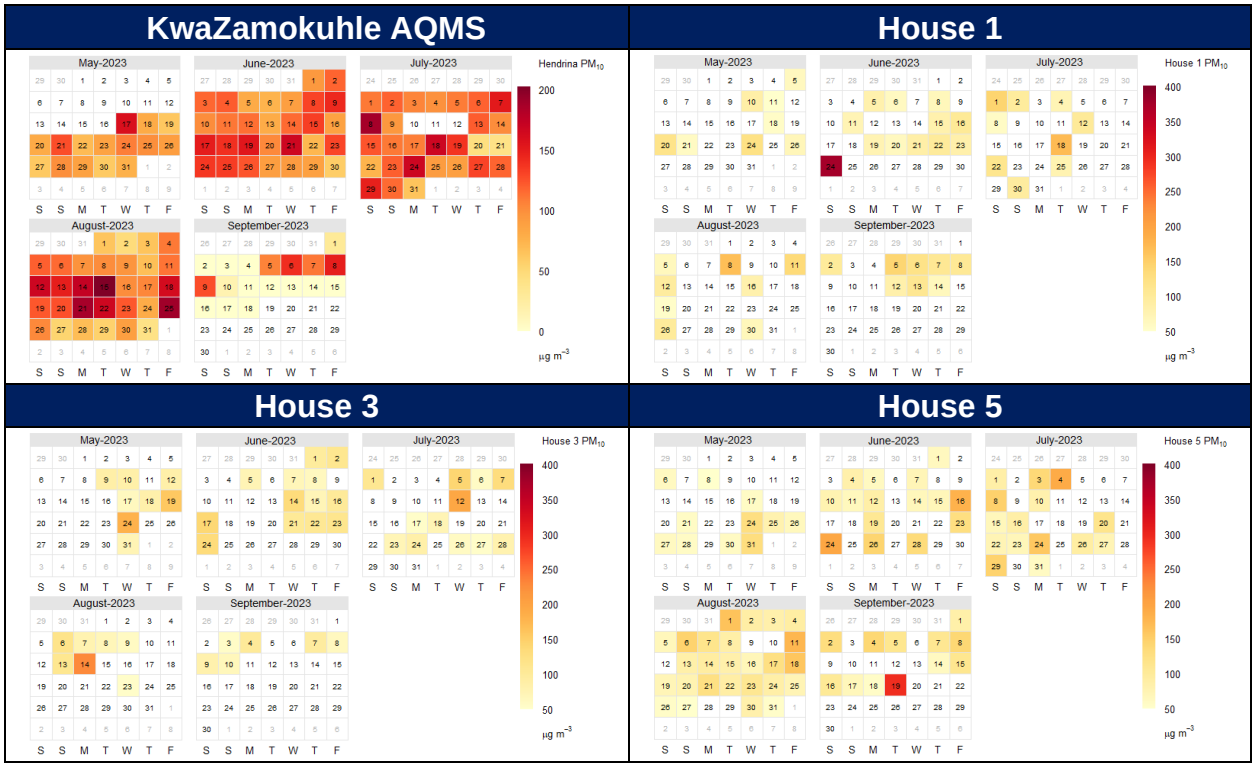

Figure 17: Daily ambient PM_{10} concentrations (µg/m^3) measured at the sampling sites during the sampling survey.

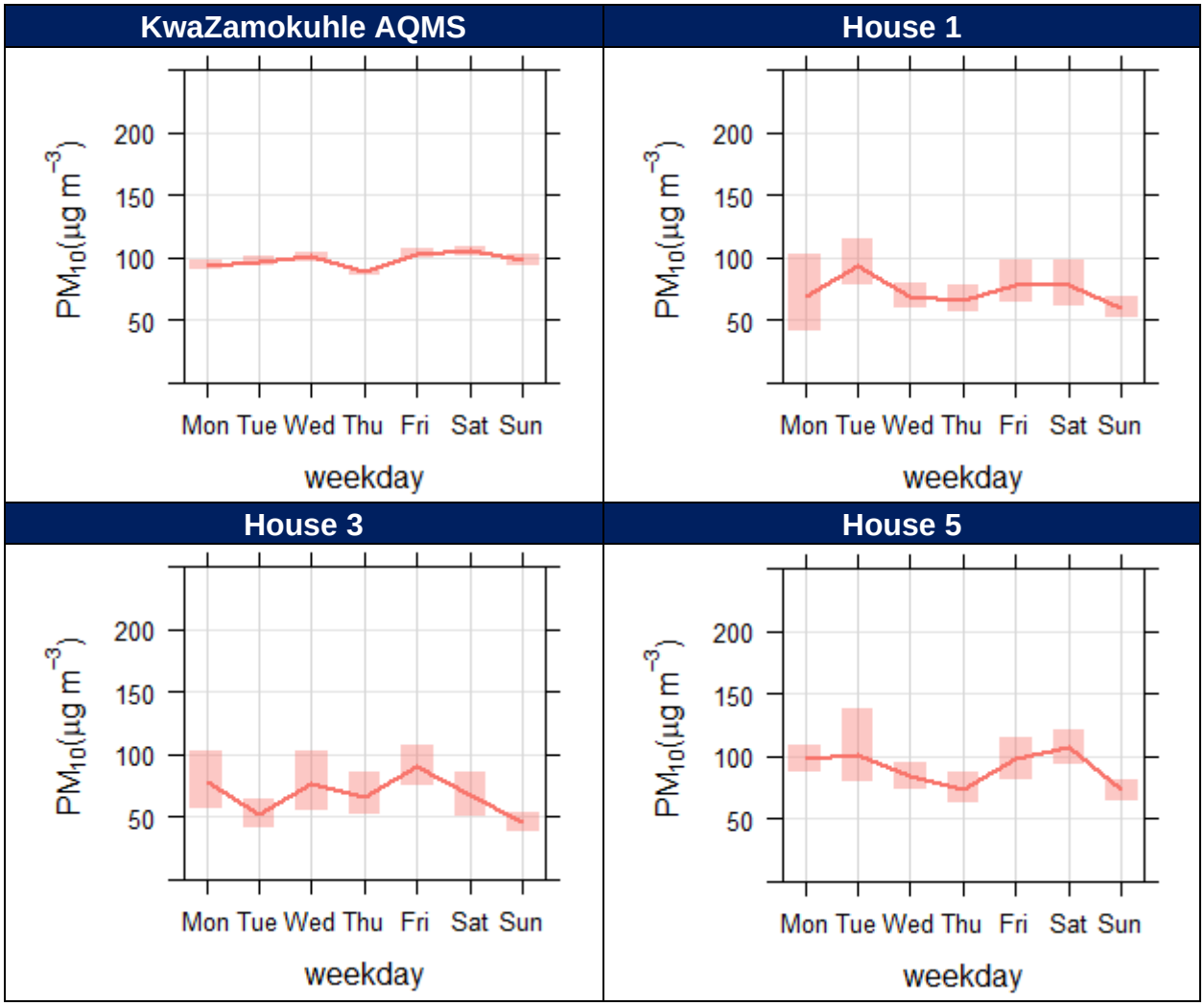

Figure 18: Average weekday ambient PM_{10} concentrations (µg/m^3) measured at sampling sites during the sampling survey.

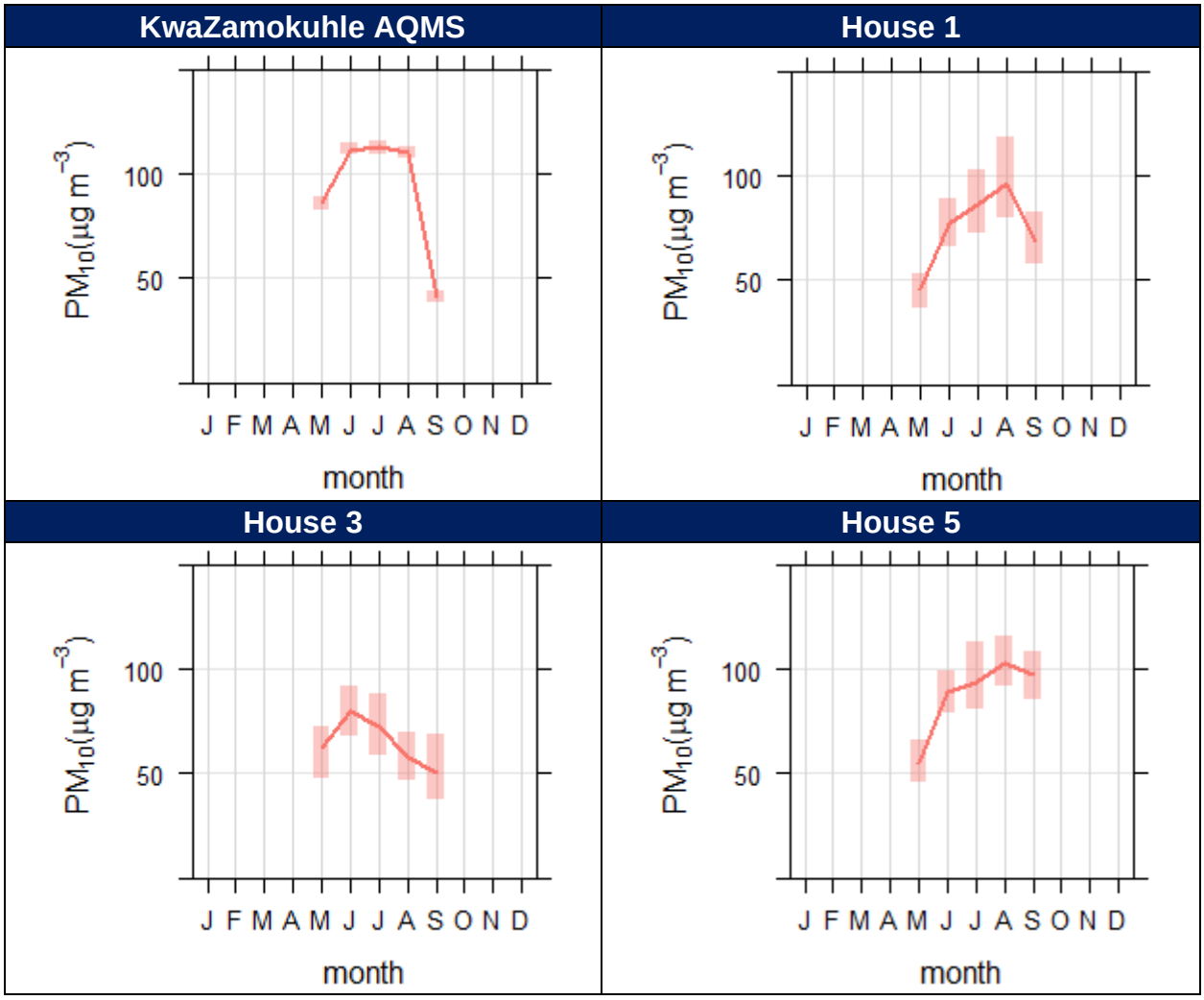

Figure 19: Monthly mean ambient PM_{10} concentrations (µg/m^3) measured at sampling sites during the sampling survey.

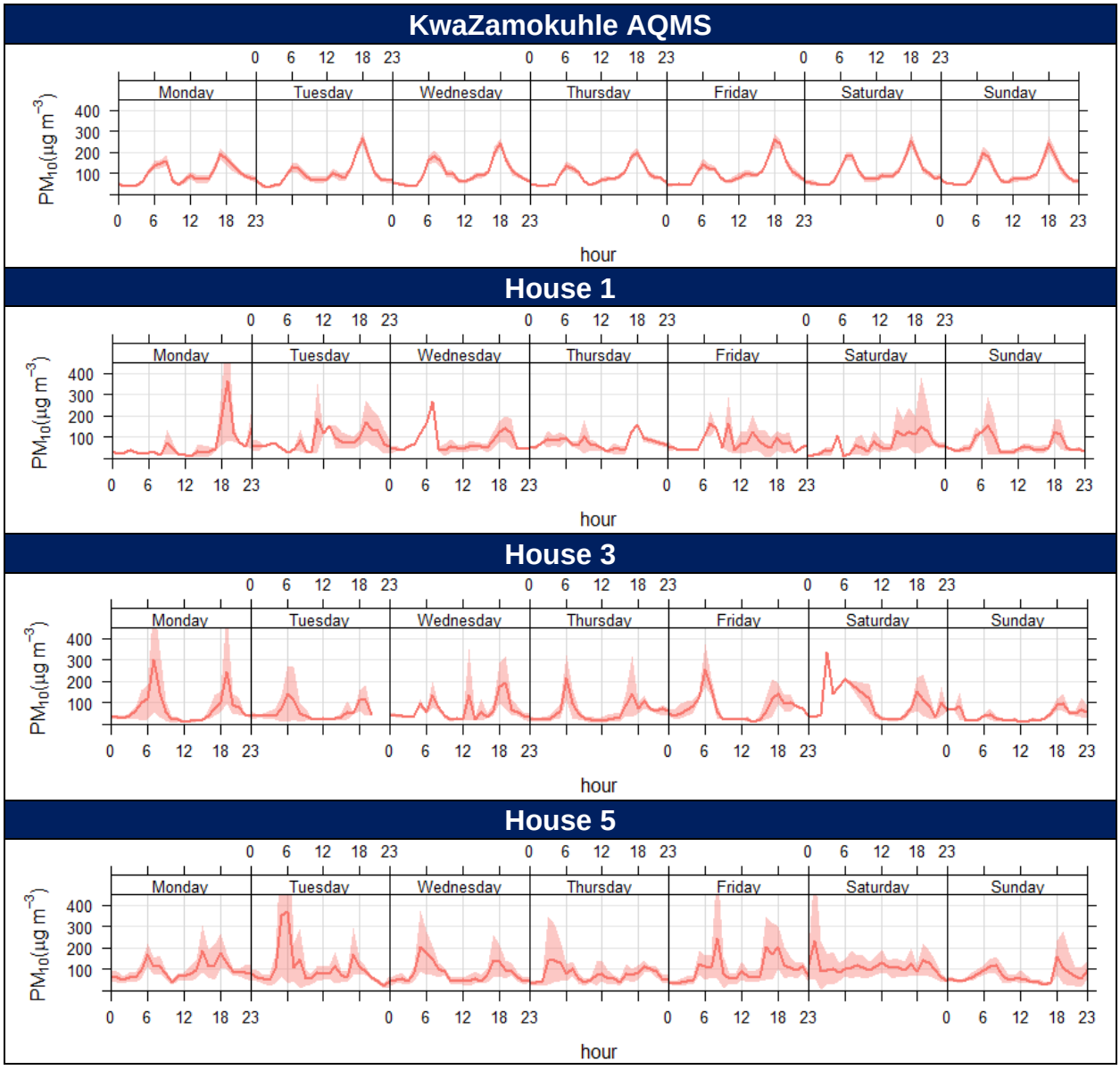

Figure 20: Weekly diurnal PM_{10} concentrations (µg/m^3) measured at the sampling sites during the sampling survey.

3.2.2 PARTICULATE MATTER ($PM_{2.5}$)

Figure 21 indicate the ambient hourly $PM_{2.5}$ concentrations recorded at the House 2 and House 4 sampling sites. Although no NAAQS exist for hourly $PM_{2.5}$ concentrations, Figure 21 highlight maximum hourly concentrations of 550 $\mu g/m^3$ and 700 $\mu g/m^3$ were recorded at House 2 and House 4 respectively. Figure 22 is a graphical representation of the mean hourly $PM_{2.5}$ concentrations for the sampling period. It is evident from Figure 22 that the highest average values are recorded during hours 06:00 to 08:00, as well as 18:00 to 20:00 for both sampling locations. House 2 indicates higher concentrations during 11:00 to 12:00 for September. These diurnal profiles are also illustrated in Figure 23. The bi-modal particulate matter peak for both House 2 and House 4 (Figure 23) is a typical profile for residential fuel burning. A morning peak occurs between 06:00 and 07:00 whilst the evening peak occurs between 18:00 and 19:00. The morning peaks reduces towards midday as the inversion layer rises & improves the mixing height of the planetary boundary layer.

Figure 24 indicate the daily ambient $PM_{2.5}$ concentrations recorded at House 2 and House 4 respectively. The daily NAAQS for $PM_{2.5}$ of 40 $\mu g/m^3$ is exceeded multiple times at both sampling sites. Both House 2 and House 4 recorded maximum daily $PM_{2.5}$ concentrations of around 150 $\mu g/m^3$. These elevated daily concentrations are indicated in the calendar plots (Figure 25). These elevated concentrations could be attributed to colder ambient temperatures leading to an increase in residential fuel burning.

Figure 26 highlights the mean weekday ambient $PM_{2.5}$ concentrations. Both House 2 and House 4 reported daily concentrations of 50 $\mu g/m^3$, with House 2 indicating higher concentrations on a Saturday.

Figure 27 illustrates the mean monthly ambient $PM_{2.5}$ concentrations recorded at House 2 and House 4 sampling sites. Both sampling locations indicate an increase from May to June, as well as a decrease from August to September.

As mentioned previously, the bi-modal particulate matter peak for both House 2 and House 4 (Figure 23) is a typical profile for residential fuel burning. These peaks are evident in Figure 28 illustrating the weekly diurnal ambient $PM_{2.5}$ concentrations. A morning peak occurs between 06:00 and 07:00 whilst the evening peak occurs between 18:00 and 19:00.

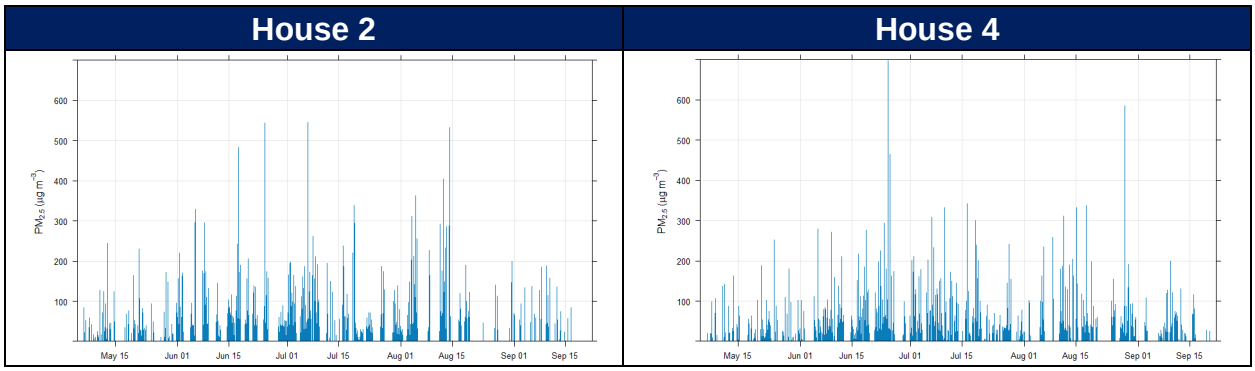

Figure 21: Hourly ambient $PM_{2.5}$ concentrations ($\mu g/m^3$) measured at the sampling sites during the sampling survey.

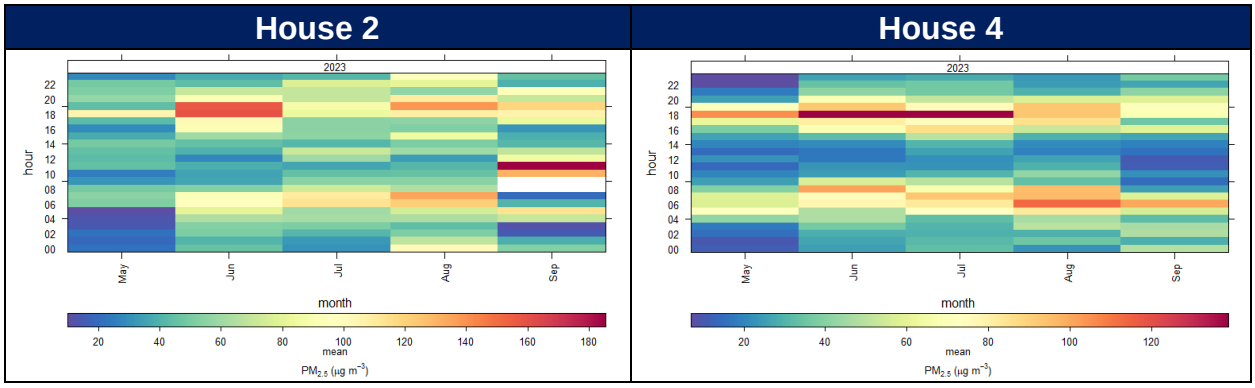

Figure 22: Mean hourly ambient $PM_{2.5}$ concentrations (µg/m^3) measured at the sampling sites during the sampling survey.

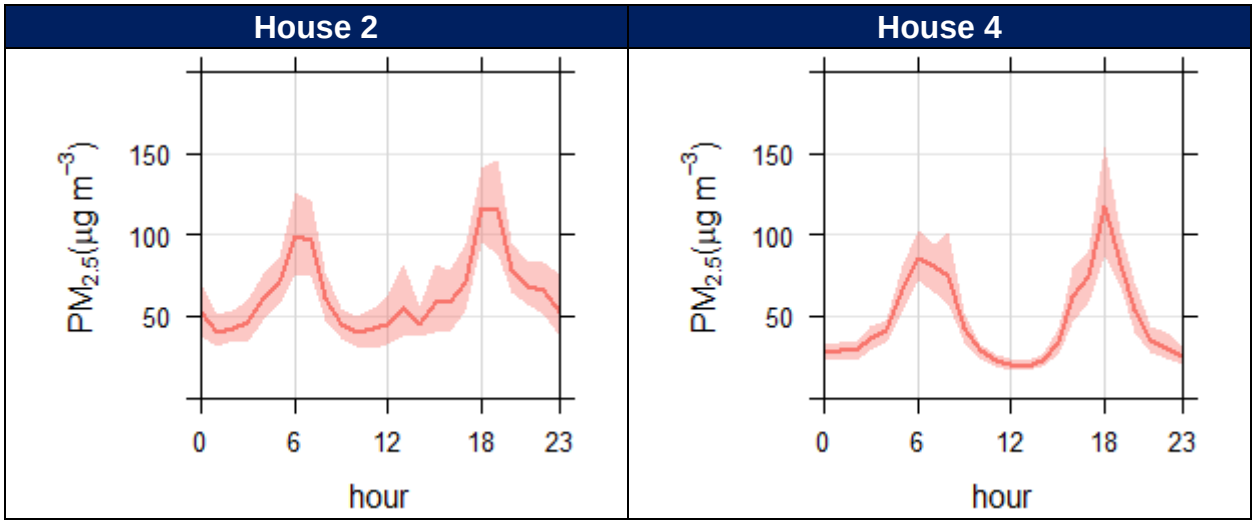

Figure 23: Hourly diurnal $PM_{2.5}$ concentrations (µg/m^3) measured at the sampling sites during the sampling survey.

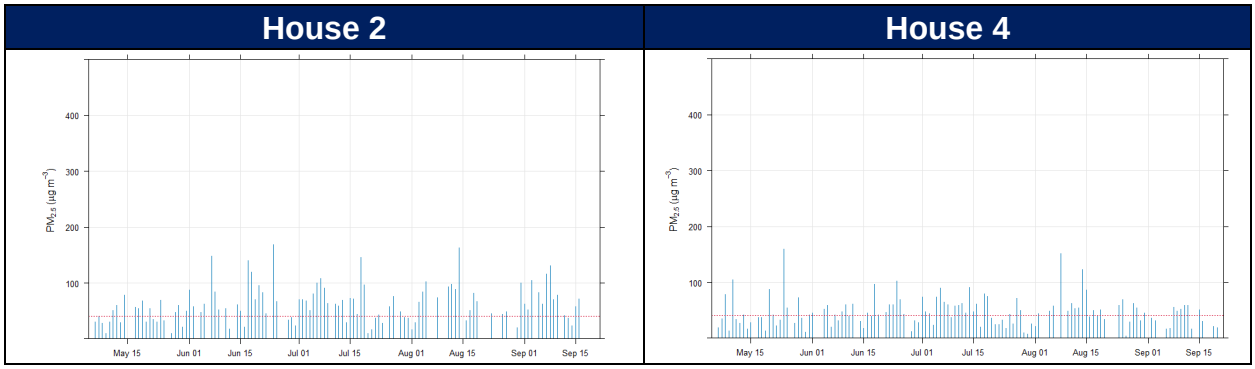

Figure 24: Daily ambient $PM_{2.5}$ concentrations (µg/m³) measured at the sampling sites during the sampling survey.

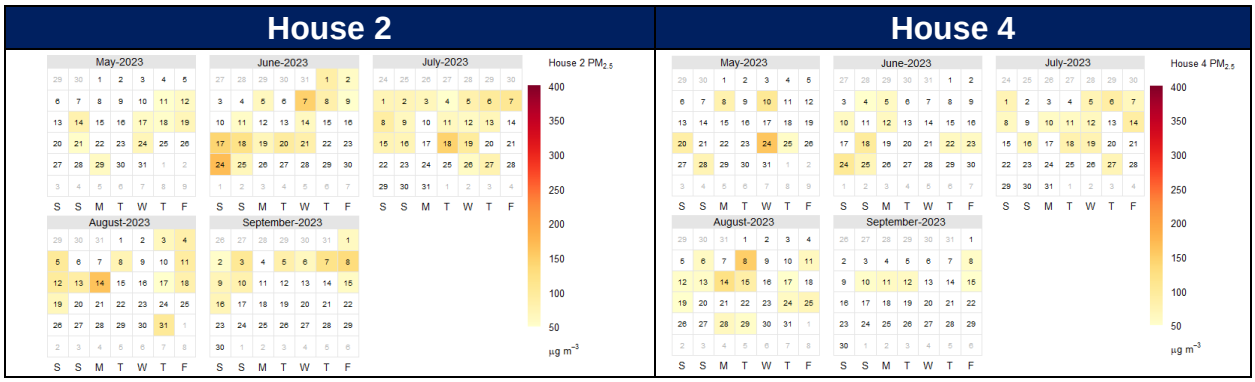

Figure 25: Daily ambient $PM_{2.5}$ concentrations (µg/m³) measured at the sampling sites during the sampling survey.

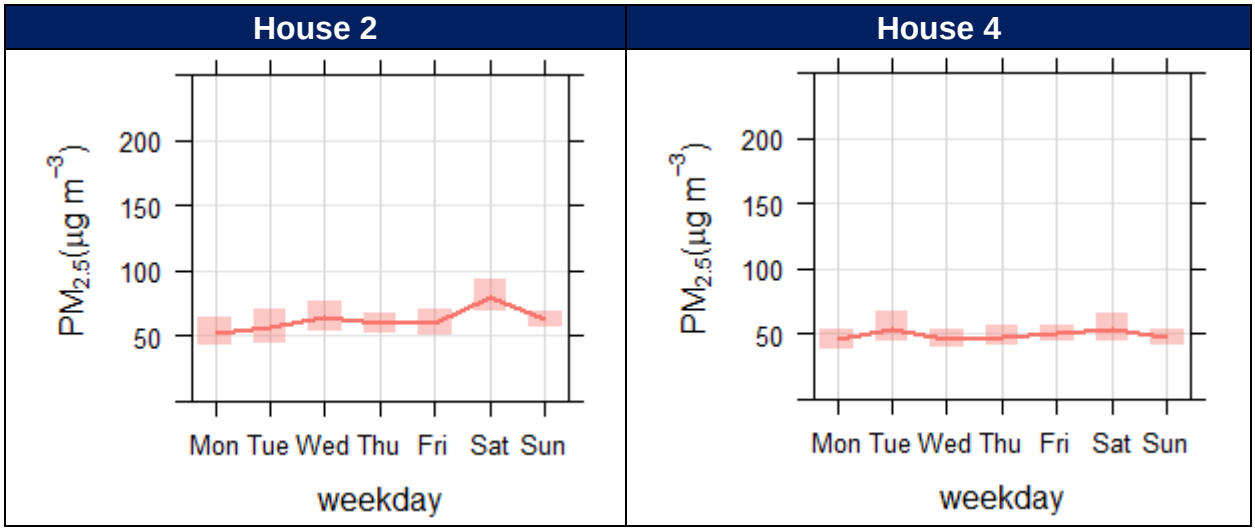

Figure 26: Weekday ambient $PM_{2.5}$ concentrations (µg/m^3) measured at the sampling sites during the sampling survey.

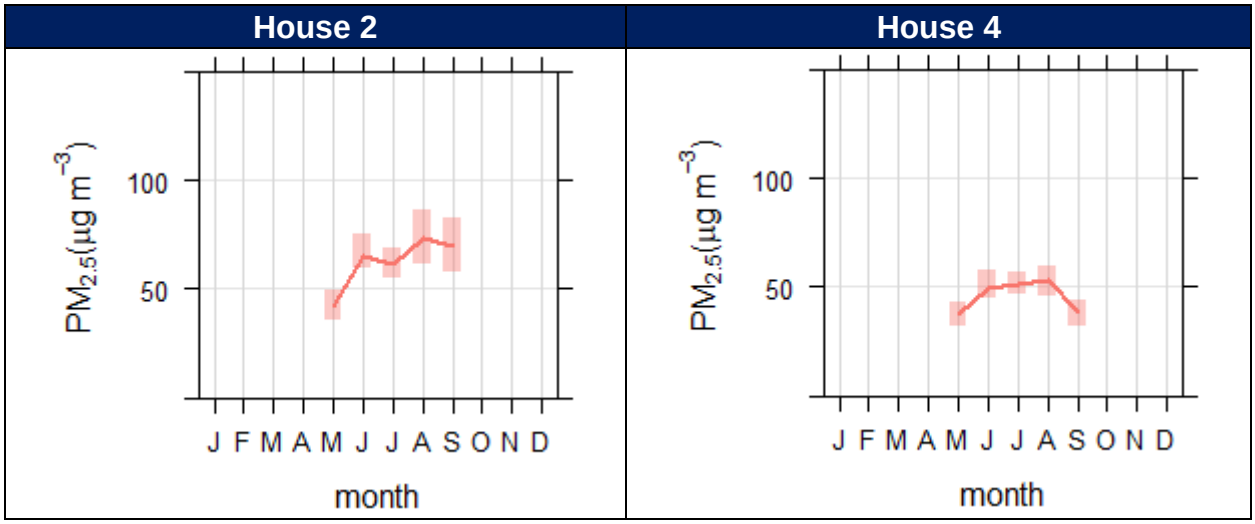

Figure 27: Mean monthly ambient $PM_{2.5}$ concentrations (µg/m^3) measured at sampling sites during the sampling survey.

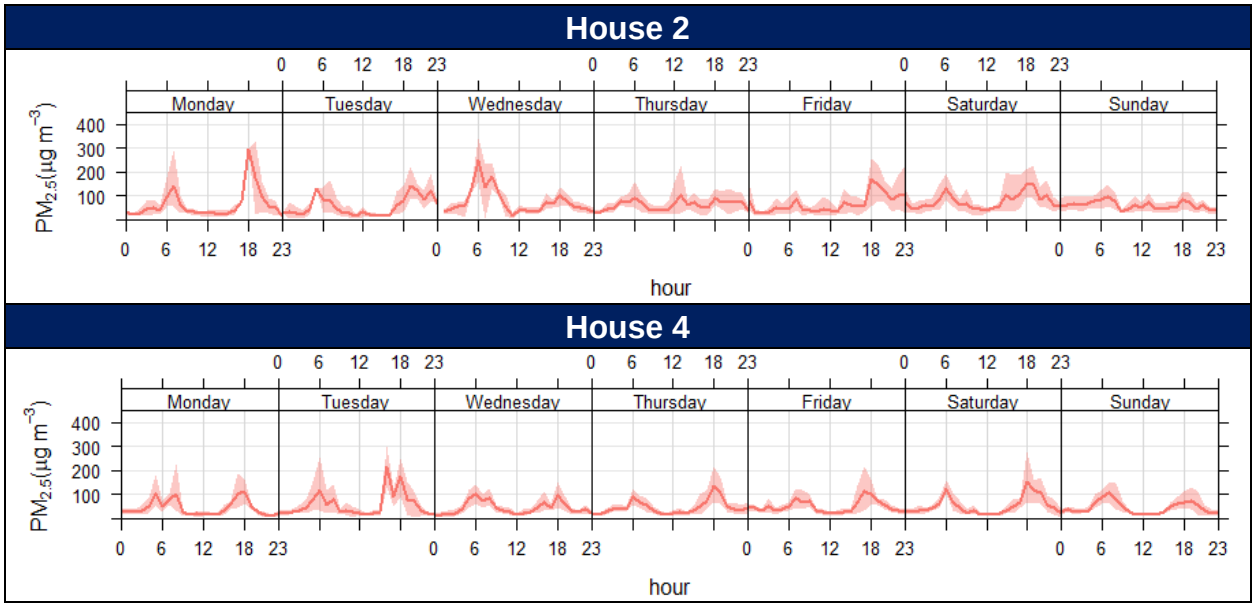

Figure 28: Weekly diurnal $PM_{2.5}$ concentrations (µg/m³) measured at sampling sites during the sampling survey.

3.2.3 SULPHUR DIOXIDE (SO_2)

Figure 29 indicate the hourly ambient SO_2 concentrations recorded at the Eskom KwaZamokuhle AQMS. The NAAQS for hourly SO_2 concentrations is 134ppb. One exceedance of the hourly NAAQS was recorded for an hourly time average for the KwaZamokuhle AQMS station during June 2023.

Figure 30 is a graphical representation of the mean hourly SO_2 concentrations for the sampling period. It is evident from Figure 30 that the highest mean concentrations were recorded between hours 17:00 to 18:00 for the KwaZamokuhle AQMS. These diurnal profiles are also illustrated in Figure 31. Figure 31 is indicative of the impact of residential fuel burning emissions.

Figure 32 indicate the daily ambient SO_2 concentrations recorded at the Eskom KwaZamokuhle AQMS. No exceedances of the daily NAAQS for SO_2 were recorded for the stations during the sampling period. Daily maximum SO_2 concentrations of 30 ppb were recorded. Figure 32 also indicate lower daily SO_2 concentrations during September compared to September. These lower daily concentrations in September could be related to lower domestic fuel burning practices that have a direct impact on the Eskom KwaZamokuhle AQMS. These daily concentrations are indicated in calendar plots (Figure 33). KwaZamokuhle AQMS indicate lower concentrations for September, compared to June, and the decrease could be attributed to colder ambient temperatures leading to an increase in residential fuel burning in the winter months.

Figure 34 highlights the mean weekday and mean monthly ambient SO_2 concentrations. The Eskom KwaZamokuhle AQMS indicates higher recorded ambient concentrations on Friday, Saturday and Sundays (weekend). The stations also illustrate a decrease in monthly concentrations from June to September.

Figure 35 is indicative of the mean weekly SO_2 concentrations. Figure 35 highlights a consistent peak throughout the entire week at 18:00. A comparison of the trend level plot for the KwaZamokuhle AQMS (Figure 30) clearly indicates that the 18:00 peak occurs in the winter months (June and July) thus indicating the impact of residential fuel burning emissions.

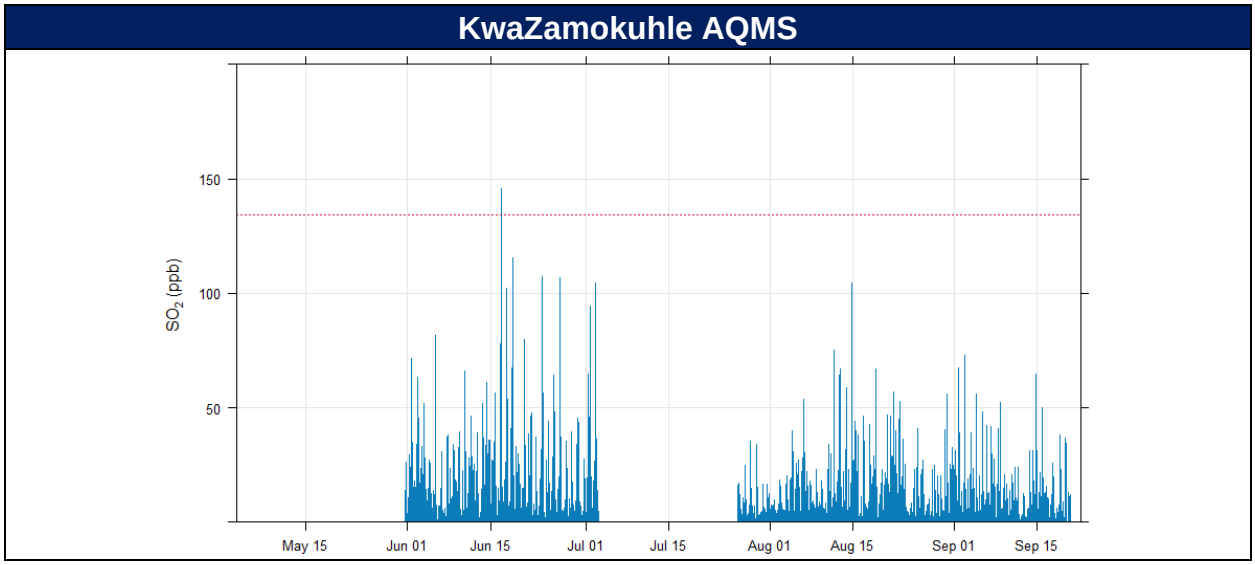

Figure 29: Hourly ambient SO_2 concentrations (ppb) measured at the Eskom KwaZamokuhle AQMS during the sampling survey (Hourly SO_2 NAAQS = 134ppb).

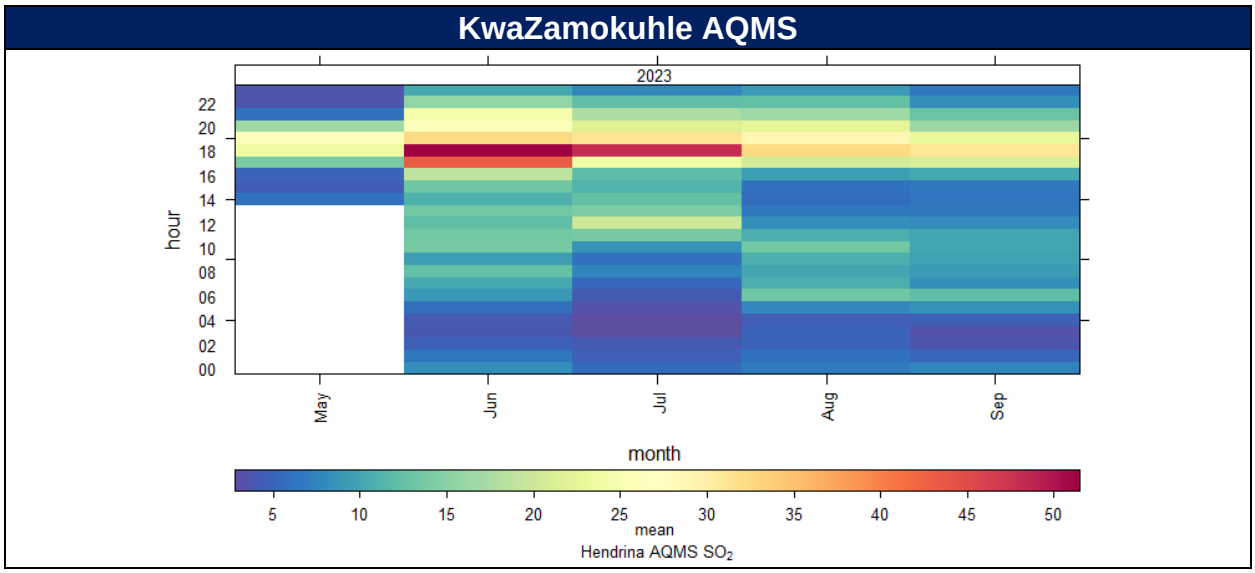

Figure 30: Hourly mean ambient SO_2 concentrations (ppb) measured at the Eskom KwaZamokuhle AQMS during the sampling survey (Hourly SO_2 NAAQS = 134ppb).

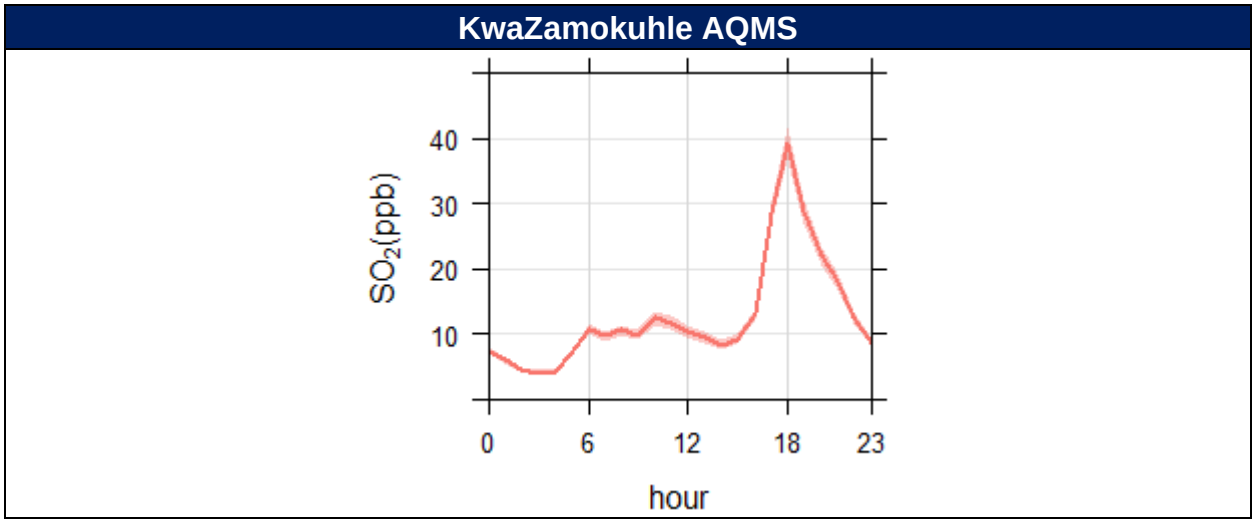

Figure 31: Mean hourly diurnal ambient SO_2 concentrations (ppb) measured at the Eskom KwaZamokuhle AQMS during the sampling survey.

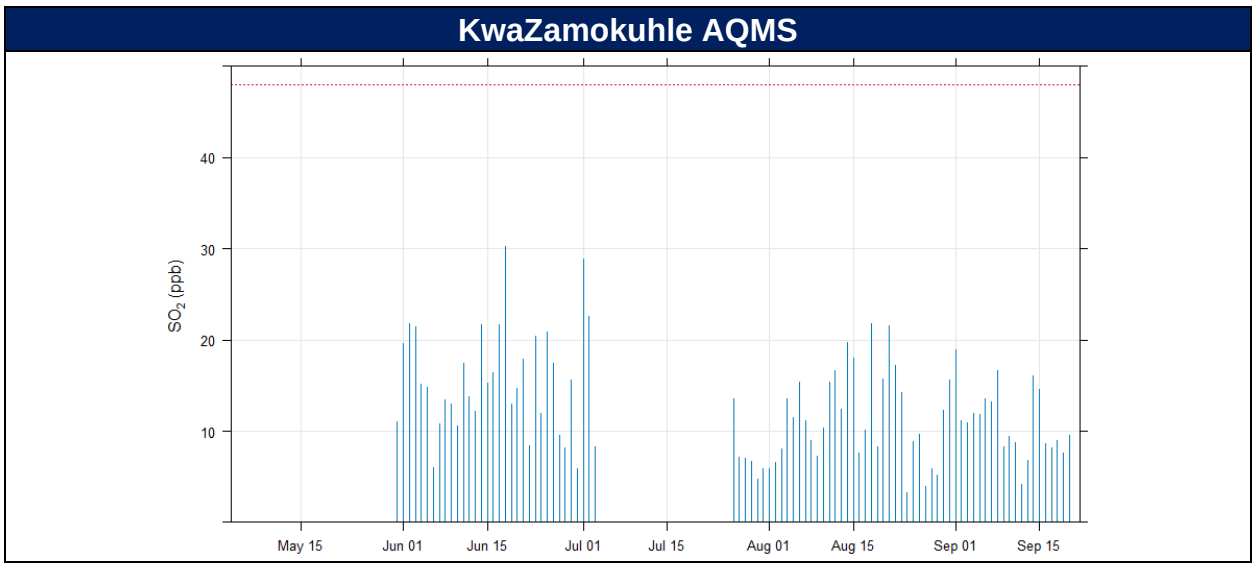

Figure 32: Daily ambient SO_2 concentrations (ppb) measured at the Eskom KwaZamokuhle AQMS during the sampling survey (Daily SO_2 NAAQS = 48ppb).

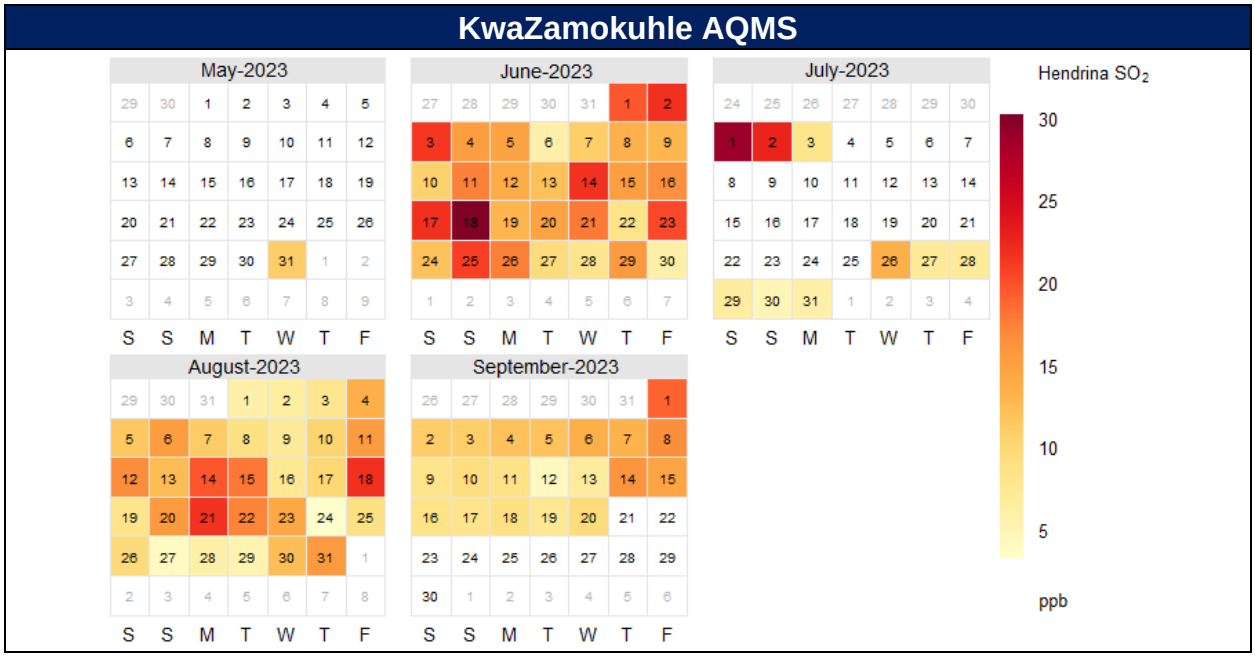

Figure 33: Daily ambient SO_2 concentrations (ppb) measured at the Eskom KwaZamokuhle AQMS during the sampling survey (Hourly SO_2 NAAQS = 48ppb).

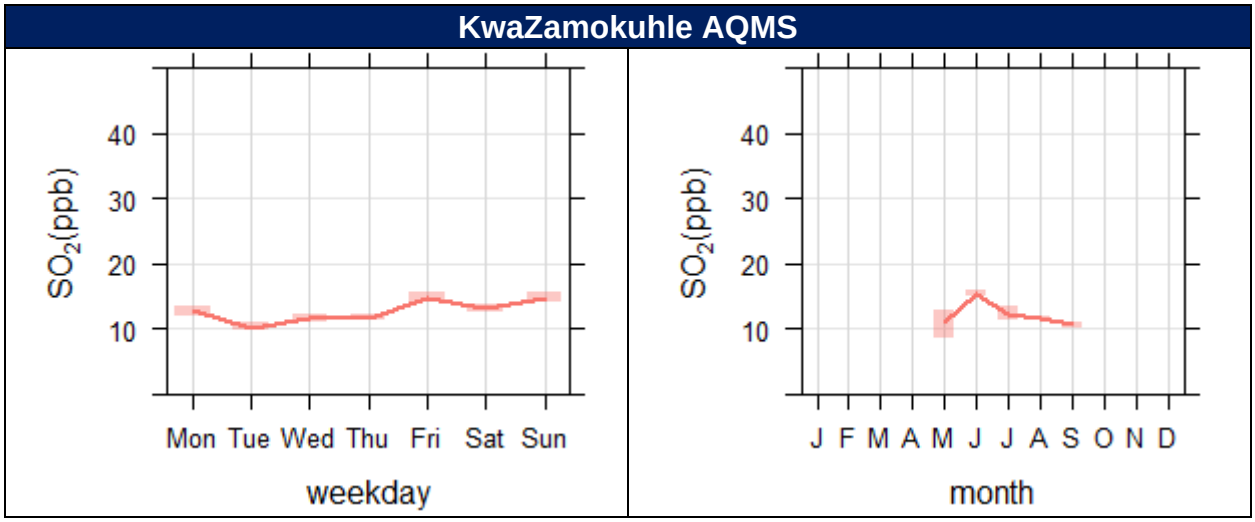

Figure 34: Mean weekday and mean monthly ambient SO_2 concentrations (ppb) measured at Eskom KwaZamokuhle AQMS during the sampling survey.

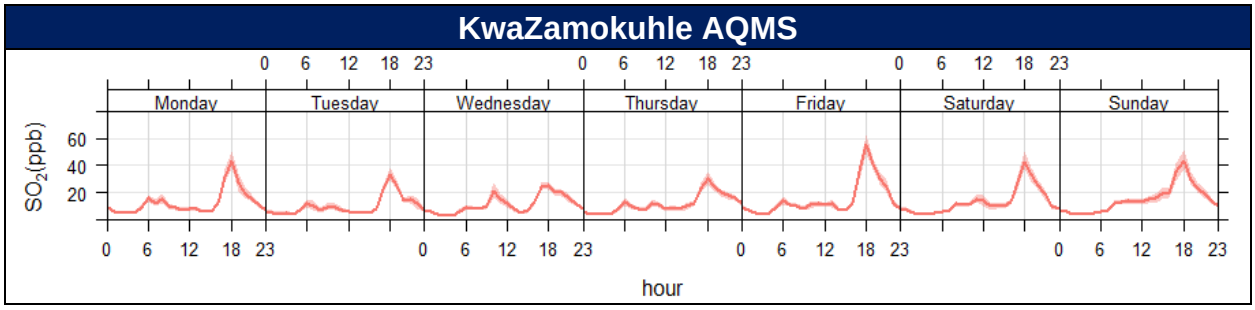

Figure 35: Weekly diurnal SO_2 concentrations (ppb) measured at the Eskom KwaZamokuhle AQMS during the sampling survey.

3.2.4 Nitrogen Dioxide (NO_2)

Figure 36 indicate the hourly ambient NO_2 concentrations recorded at the Eskom KwaZamokuhle AQMS. The NAAQS for hourly NO_2 concentrations is 106ppb. No exceedances of the hourly NAAQS were recorded for an hourly time average for the station. Figure 36 highlight maximum hourly NO_2 concentrations of approximately 75ppb at the Eskom KwaZamokuhle AQMS.

Figure 37 is a graphical representation of the mean hourly NO_2 concentrations for the sampling period. It is evident from Figure 37 that elevated concentrations were recorded during hours 06:00 to 08:00 and 17:00 to 19:00 for the Eskom KwaZamokuhle AQMS. These diurnal profiles are also illustrated in Figure 38. The Eskom KwaZamokuhle AQMS signature in Figure 38 explicitly reveal that the variability of this pollutant concentration is conditioned by vehicle emissions. The diurnal cycle corresponds to the cyclical nature of traffic volume with marked peaks in concentration on weekdays around the early-morning and late-afternoon rush-hours.

Figure 39 indicate the daily ambient NO_2 concentrations recorded at the Eskom KwaZamokuhle AQMS. No daily NAAQS for NO_2 exists. Daily maximum NO_2 concentrations of approximately 30 ppb were recorded. These daily mean NO_2 concentrations are graphically presented in Figure 40.

Figure 40 highlights the mean weekday and mean monthly ambient NO_2 concentrations. A slight increase was recorded for Fridays, as well as a decrease in monthly concentrations from June to September.

Figure 41 is indicative of the mean weekly NO_2 concentrations. It is evident for the Eskom KwaZamokuhle AQMS that the weekly diurnal cycle corresponds to the cyclical nature of traffic volume with marked peaks in concentration on weekdays around the early-morning and late-afternoon rush-hours.

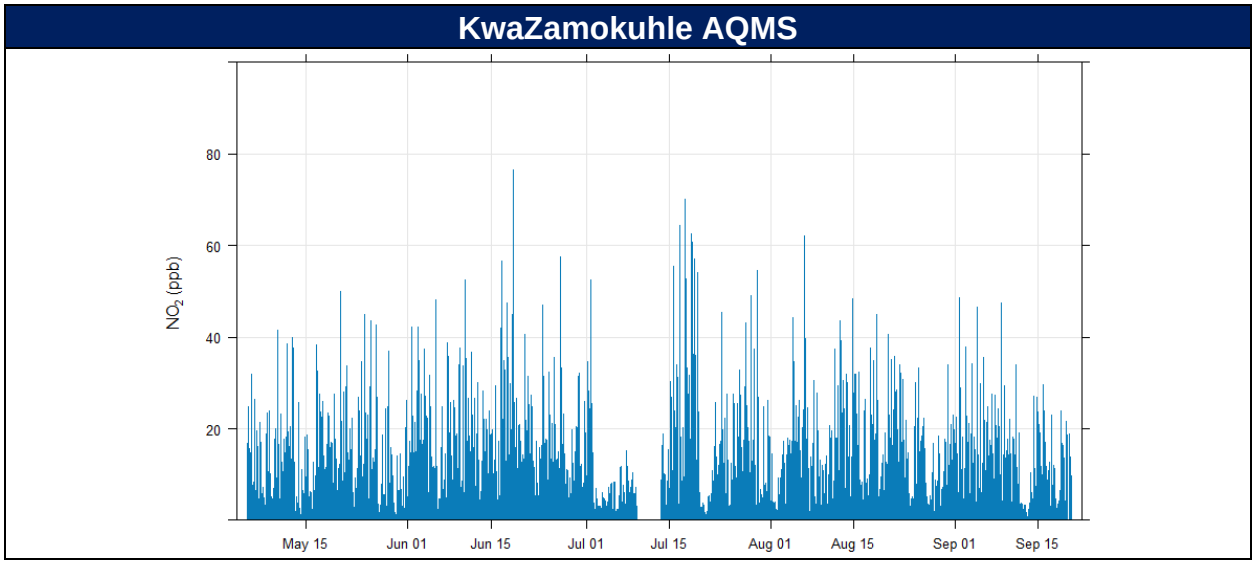

Figure 36: Hourly ambient NO_2 concentrations (ppb) measured at the Eskom KwaZamokuhle AQMS during the sampling survey (Hourly NO_2 NAAQS = 106ppb).

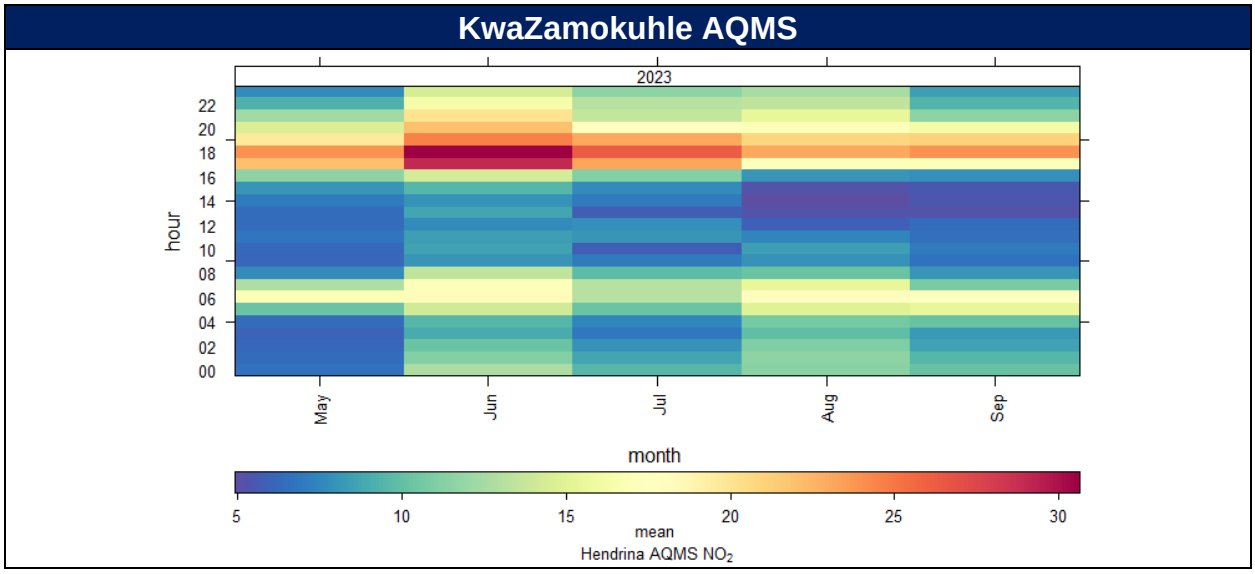

Figure 37: Hourly mean ambient NO_2 concentrations (ppb) measured at the Eskom KwaZamokuhle AQMS during the sampling survey (Hourly NO_2 NAAQS = 106ppb).

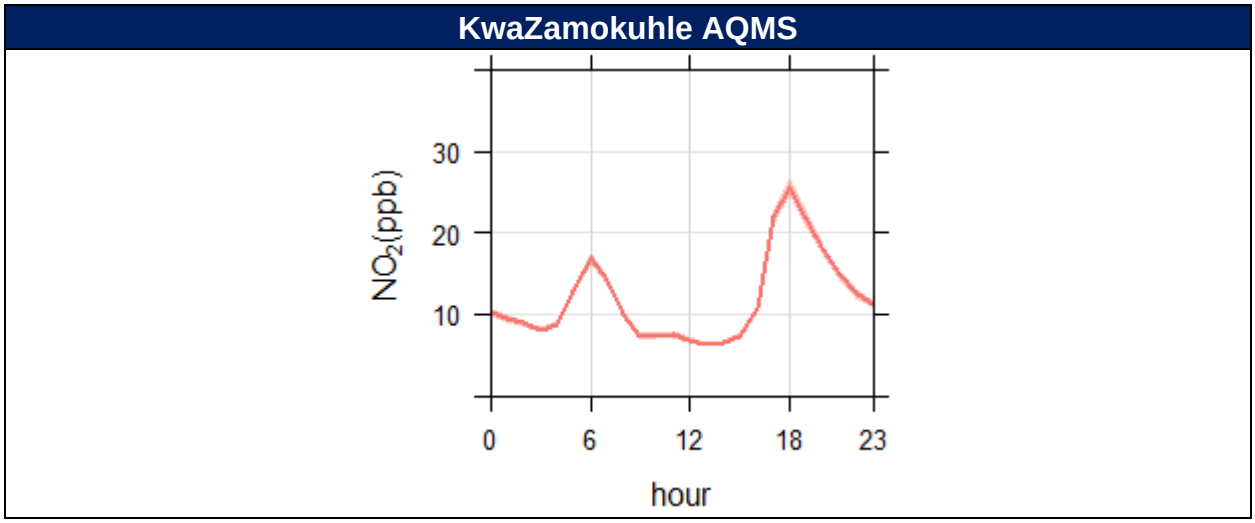

Figure 38: Mean hourly diurnal NO_2 concentrations (ppb) measured at the Eskom KwaZamokuhle AQMS sites during the sampling survey.

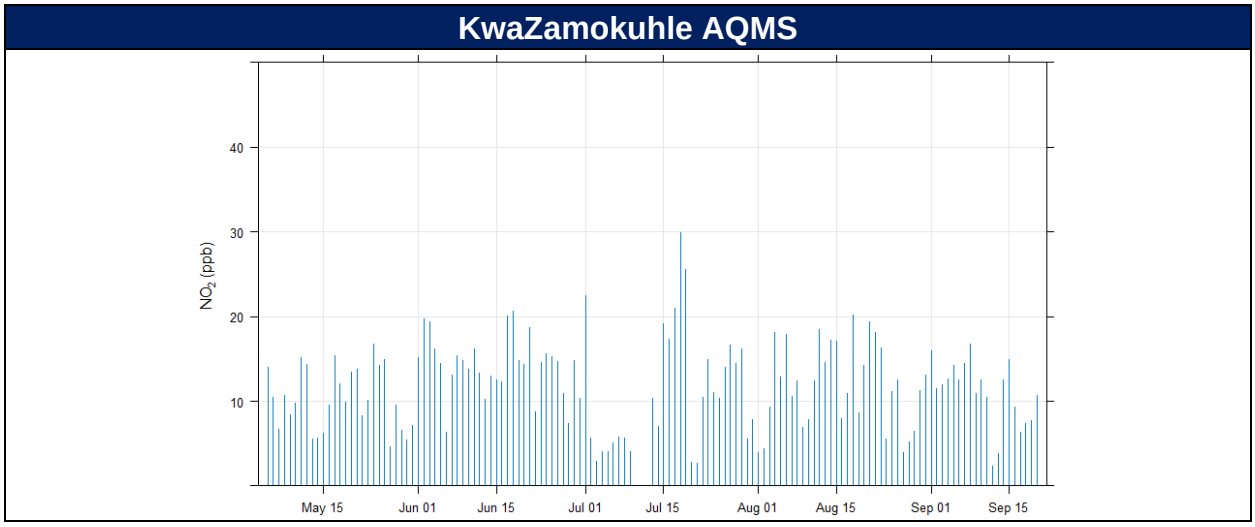

Figure 39: Daily ambient NO_2 concentrations (ppb) measured at the Eskom KwaZamokuhle AQMS during the sampling survey

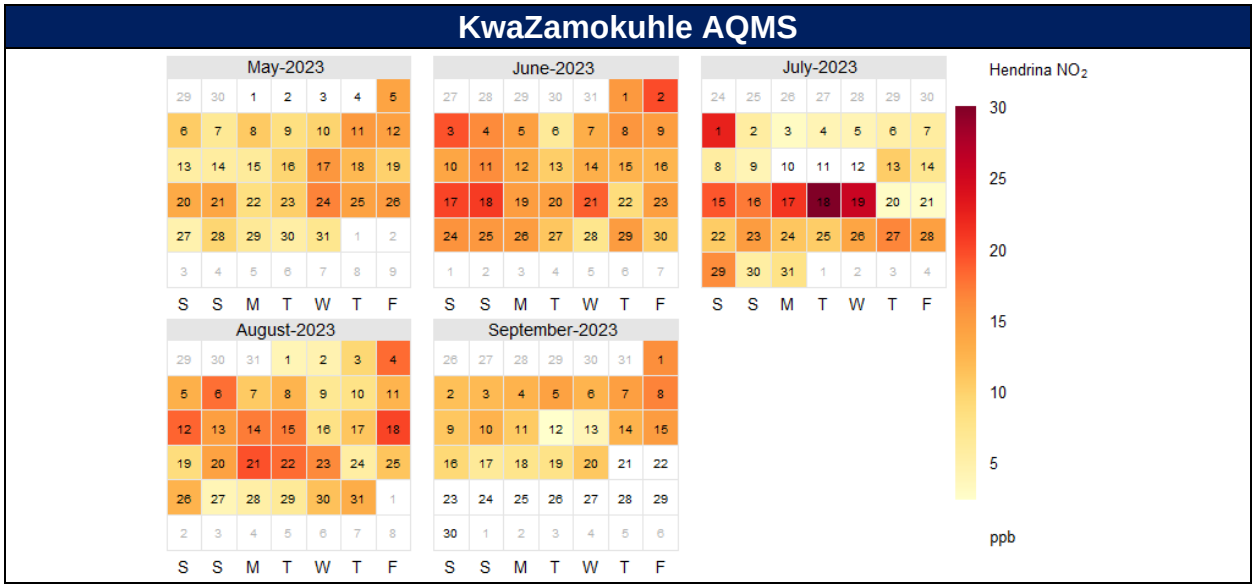

Figure 40: Daily ambient NO_2 concentrations (ppb) measured at the Eskom KwaZamokuhle AQMS during the sampling survey

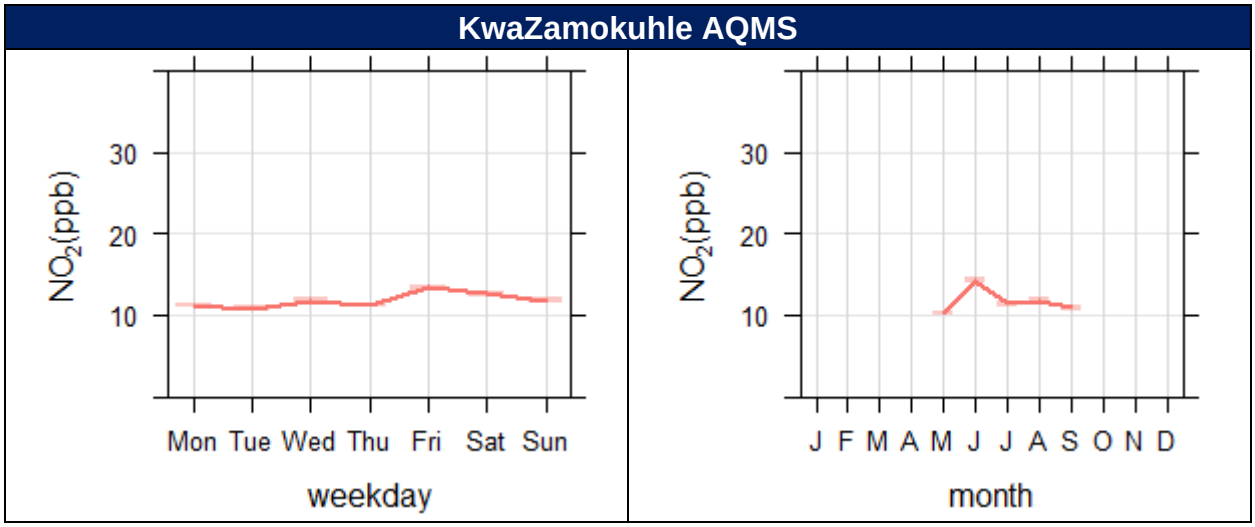

Figure 41: Mean weekday and mean monthly ambient NO_2 concentrations (ppb) measured at the Eskom KwaZamokuhle AQMS during the sampling survey.

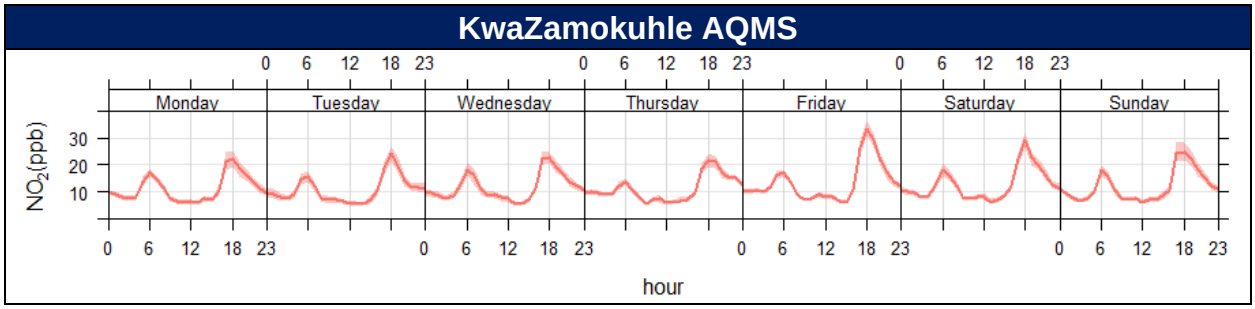

Figure 42: Weekly diurnal NO_2 concentrations (ppb) measured at the Eskom KwaZamokuhle AQMS during sampling survey.

4.3 EMISSION SOURCE CONTRIBUTION

The emission performance of an individual air-pollution source can be inferred from an ambient record by isolating its signal of impacts. However, ambient data are not conventionally used for such purposes because individual signals tend to be modified, obscured, or complicated by confounding factors (Szulecka et al., 2017). However, more detailed and source-specific information can be extracted if analyses are performed using a subset of the data that has been "conditionally-selected" to exclude superimposed impacts from non-relevant sources (Malby et al., 2013). Numerous studies (Carslaw, 2007; Griffin et al., 2009; Malby et al., 2008; Shu et al., 2017) have demonstrated that these signals can successfully be used for source attribution. A common method for source characterisation is the use of pollution roses and bivariate polar plots (Carslaw et al., 2006; Westmoreland et al., 2007; Carslaw and Beevers, 2013; Uria Tellaetxe and Carslaw, 2014).

Bivariate polar plots have proved to be extremely valuable for identifying and understanding sources of air pollution (Carslaw et al., 2006; Westmoreland et al., 2007). Bivariate polar plots provide an effective graphical means of discriminating different source types and characteristics as these plots show how the concentration of a pollutant varies by two different variables at a specific receptor.

4.3.1 POLLUTION ROSES

The pollution rose is useful for considering pollutant concentrations by wind direction, or more specifically the percentage time the concentration is in a particular range. This type of approach can be very informative for air pollutant species (Henry et al. 2009).

4.3.1.1 Particulate Matter (PM_{10})

Figure 43 illustrate the pollution rose for PM_{10} measured at the Eskom KwaZamokuhle AQMS. These plots are very useful for understanding which wind directions control the overall mean concentrations. The pollution rose clearly indicates that high episodes of pollutant levels are primarily related to winds from the: south- and north-westerly direction. A comparison of the annual wind rose for the Eskom KwaZamokuhle AQMS (Figure 8) to the pollution roses (Figure 43) shows higher pollutant concentrations occur at higher wind speeds. Conversely lower wind speeds (Figure 8) are associated with lower concentrations (Figure 43). It should be noted that higher wind speeds are typically associated with elevated emissions from tall stack sources whilst low-level emissions behave differently, and higher concentrations would normally be observed during weak-wind conditions.

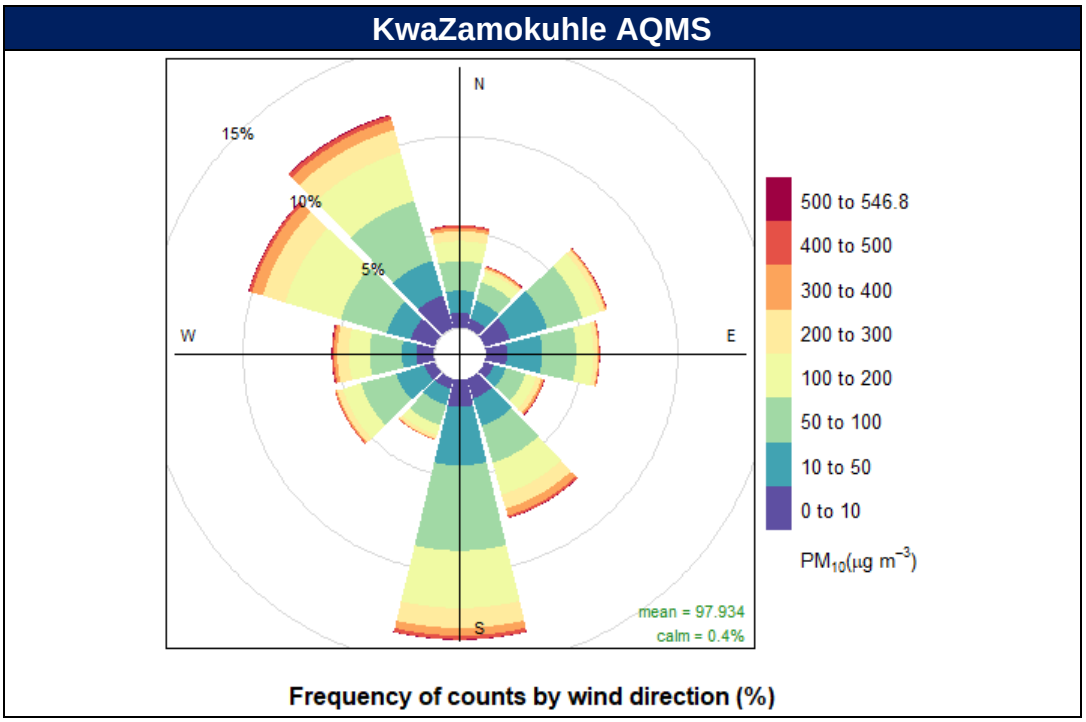

Figure 43: Pollution roses indicating which wind directions contribute most to overall mean concentrations for PM_{10}.

4.3.1.2 Sulphur Dioxide (SO_2)

Figure 44 illustrates the pollution roses for SO_2 measured at the Eskom KwaZamokuhle AQMS. The pollution rose indicates lower concentrations (0 to 50 ppb) emanating from all wind directions. Figure 44 illustrates that hourly mean concentrations of 50 to 200 ppb SO_2, recorded at the Eskom KwaZamokuhle AQMS are predominantly associated with sources emanating from a north-westerly direction. The higher concentrations could be indicative of the power stations located in a north-westerly direction from the KwaZamokuhle AQMS.

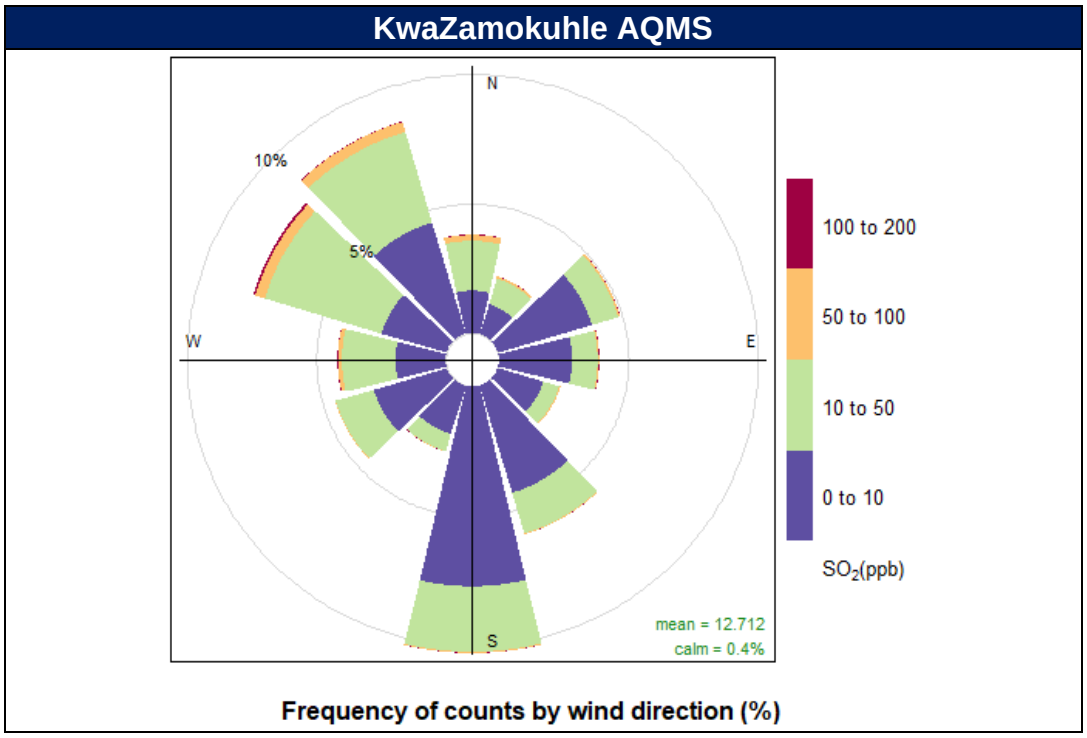

Figure 44: Pollution roses indicating which wind directions contribute most to overall mean concentrations for SO_2.

4.3.1.3 Nitrogen Oxide (NO_2)

Figure 45 illustrates the pollution roses for NO_2 measured at the Eskom KwaZamokuhle AQMS. The pollution rose indicates lower concentrations (0 to 50 ppb) emanating from all wind directions. Figure 45 illustrates those hourly mean concentrations of 50 to 200 ppb NO_2, recorded at the KwaZamokuhle AQMS are predominantly associated with sources emanating from a north-westerly direction. The higher concentrations could be indicative of the power stations located in a north-westerly direction from the KwaZamokuhle AQMS.

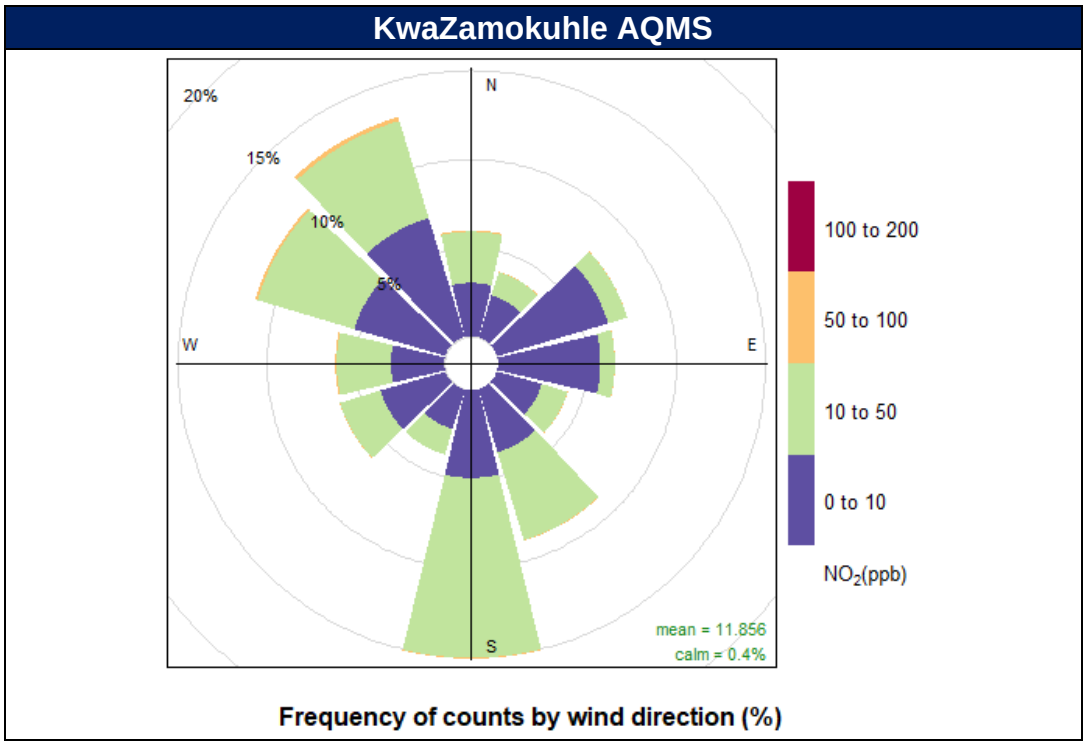

Figure 45: Pollution roses indicating which wind directions contribute most to overall mean concentrations for NO_2.

4.3.2 Bivariate Polar Plots for Mean Concentration & Wind Speed

Bivariate plots indicate how the concentration of a pollutant varies by wind direction and wind speed at a receptor. The wind speed dependence of a source can provide important information concerning the source type and characteristics (Carslaw et al., 2006; Jones et al., 2010). High ground level concentrations from tall stack emissions are more prevalent during stronger wind speeds during stable conditions whilst conversely low-level emissions, and higher concentrations would normally be observed during weak-wind conditions.

4.3.2.1 Particulate Matter (PM_{10})

Elevated particulate (PM_{10}) concentrations at the Eskom KwaZamokuhle AQMS indicate source contributions from the north-west at higher (between 8 and 10 m/s) wind speeds (Figure 46). At low wind speeds the symmetrical plot shows a localised contribution, most likely the result of residential fuel burning (Figure 46).

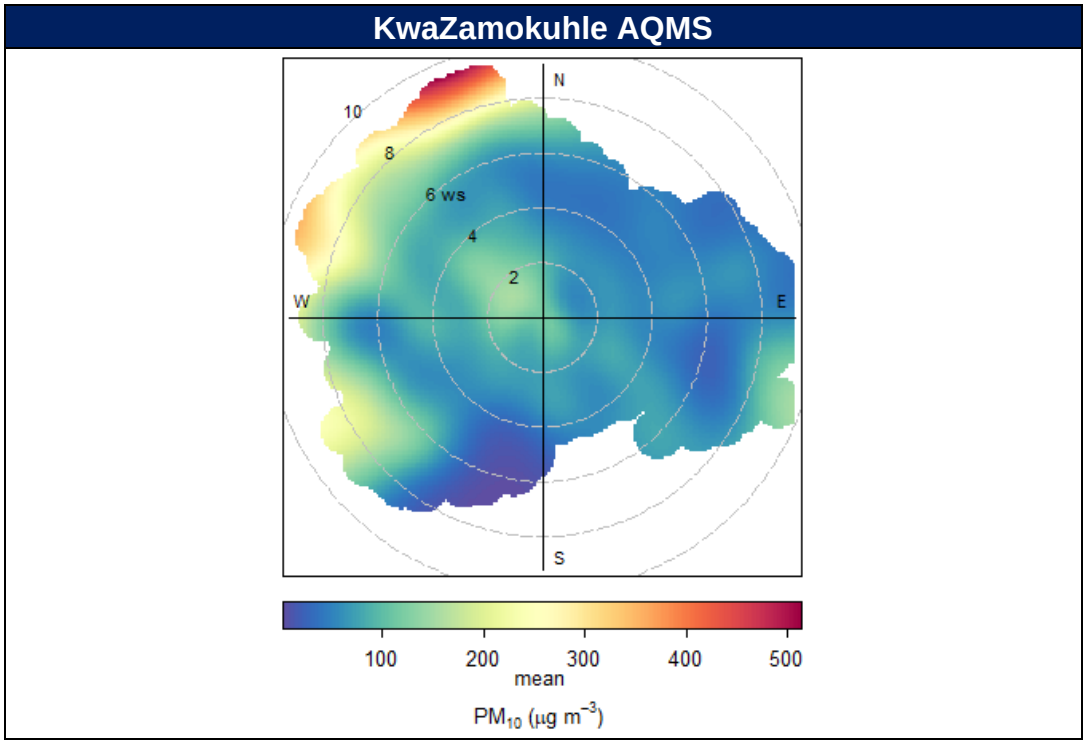

Figure 46: Polar plot of hourly mean PM_{10} concentration at the Eskom KwaZamokuhle AQMS for the sampling period.

4.3.2.2 Sulphur Dioxide (SO_2)

The SO_2 concentrations observed at the Eskom KwaZamokuhle AQMS (Figure 47) indicate source contribution from a north-westerly direction. Elevated SO_2 concentrations are evident at low wind speeds (1 to 3 m/s) indicating a local SO_2 source. This could most like be the result of residential fuel burning.

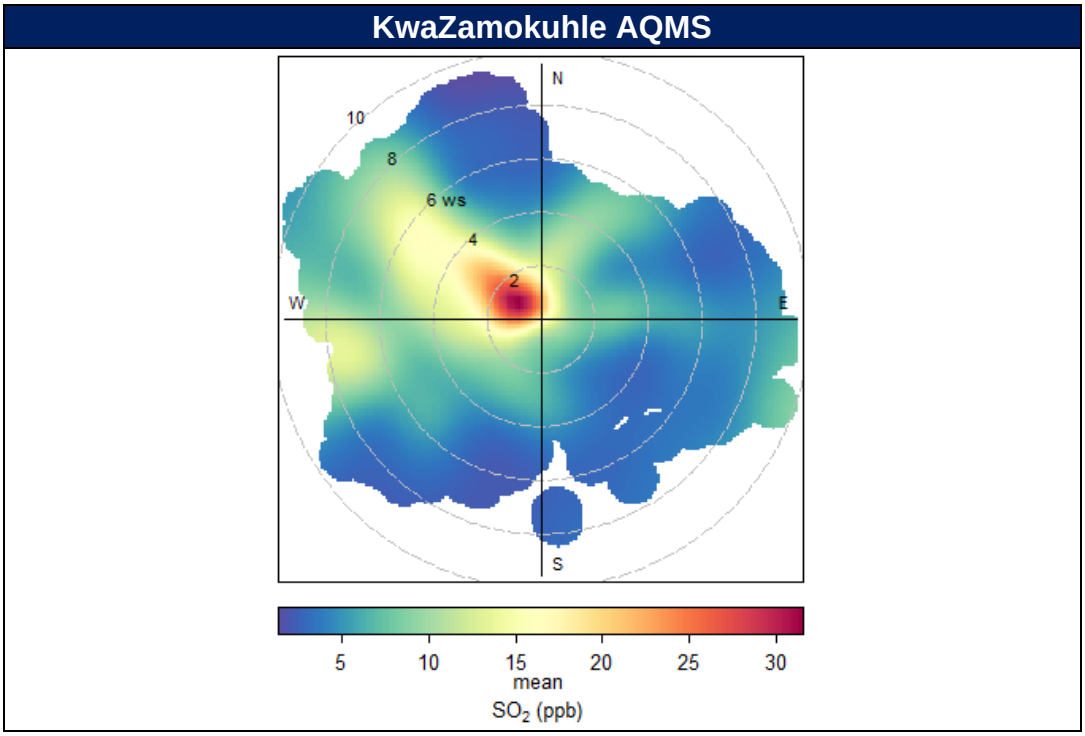

Figure 47: Polar plot of hourly mean SO_2 concentration at the Eskom KwaZamokuhle AQMS for the sampling period.

4.3.2.3 Nitrogen Dioxide (NO_2)

Figure 48 indicate the bivariate NO_2 polar plots for the Eskom KwaZamokuhle AQMS. The highest concentrations occur under very low wind speed conditions (0 to 2m/s) from the north-west. These high concentrations occur under stable atmospheric conditions when non-buoyant ground-level sources are important such as road transport emissions.

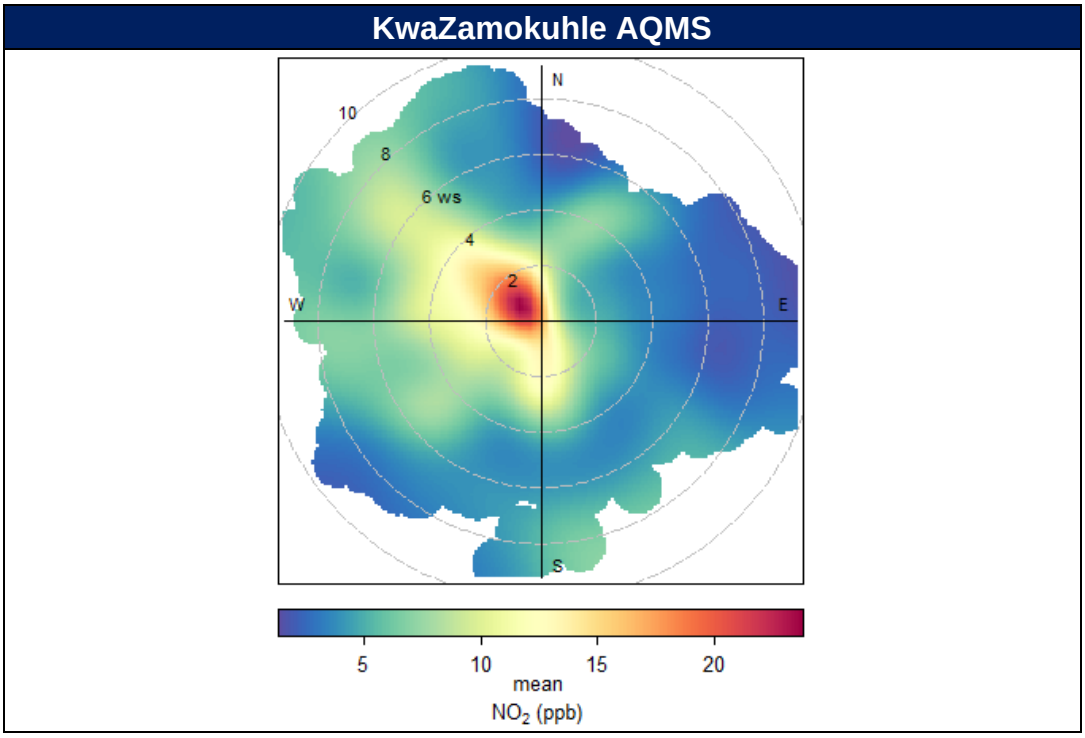

Figure 48: Polar plot of hourly mean NO_2 concentration at the Eskom KwaZamokuhle AQMS for the sampling period.

4.3.3 Bivariate Polar Plot for Mean Concentration & Temperature

These plots show how the concentration of a pollutant varies by wind direction and temperature at a receptor. Temperature can help reveal high-level sources brought down to ground level in unstable atmospheric conditions or show the effect a source emission dependent on temperature e.g., residential burning for space heating.

4.3.3.1 Particulate Matter (PM_{10})

Figure 49 indicates the bivariate polar plots for PM_{10} concentrations as a function of wind direction and surface temperature for the Eskom KwaZamokuhle AQMS. The highest concentrations occur during temperatures of 10 to 30°C in a north-westerly direction, which results mostly from residential fuel burning.

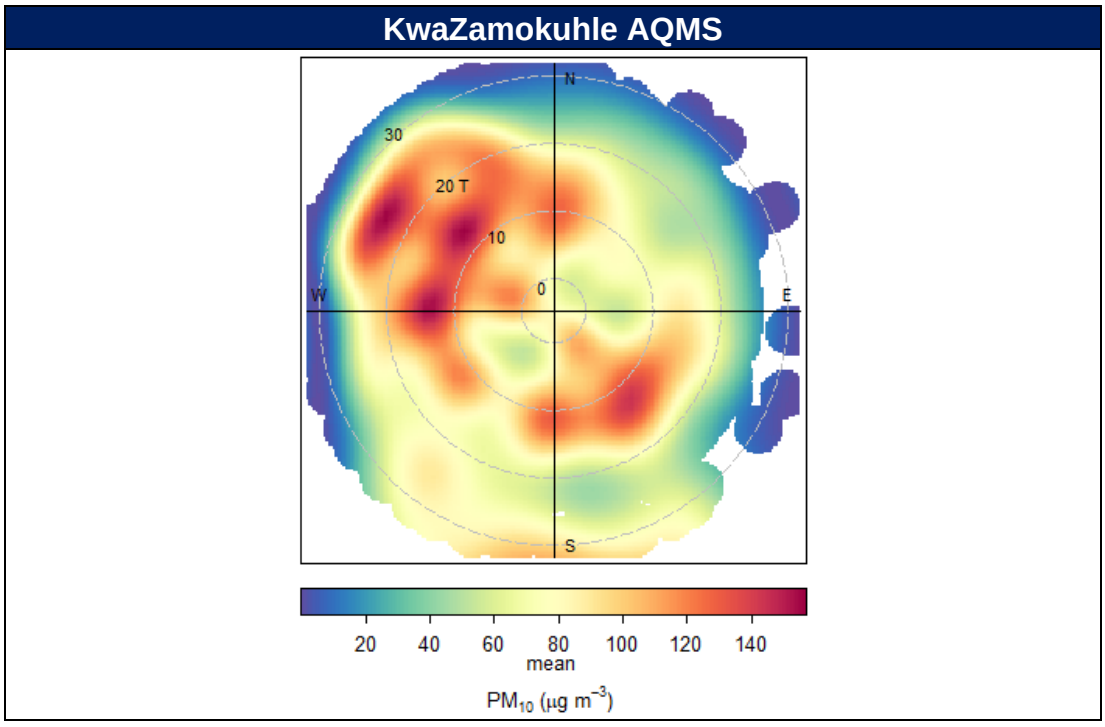

Figure 49: Polar plot of hourly mean PM_{10} concentration at the Eskom KwaZamokuhle AQMS for the sampling period.

4.3.3.2 Sulphur Dioxide (SO_2)

Figure 48 indicate the bivariate polar plot for hourly SO_2 concentrations as a function of wind direction and surface temperature. The bivariate polar plot (Figure 48) indicates an area of high concentration to the north-west that occur at higher temperatures (10 to 20°C), possibly corresponding to the activities of the power stations located towards a north-westerly direction relative to the KwaZamokuhle AQMS.

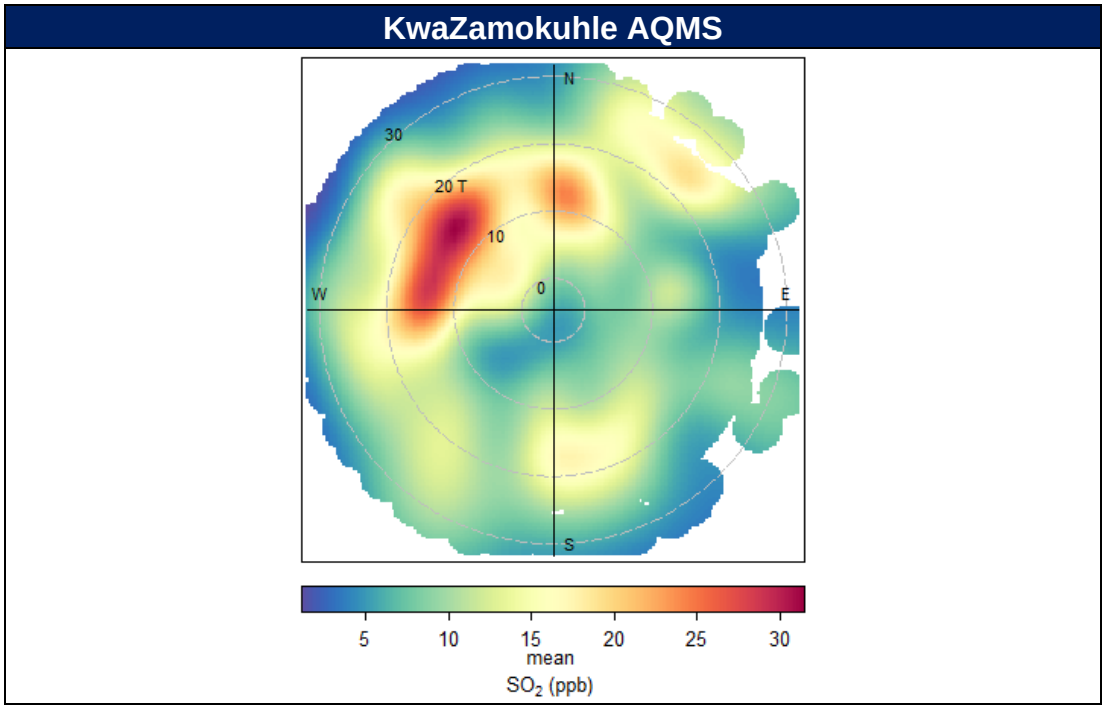

Figure 48: Polar plot of hourly mean SO_2 concentration at the Eskom KwaZamokuhle AQMS for the sampling period.

4.3.3.3 Nitrogen Dioxide (NO_2)

Figure 49 indicate the bivariate polar plot for hourly NO_2 concentrations as a function of wind direction and surface temperature. It is apparent that there is a clear dependence of NO_2 concentrations with increasing ambient temperature for the Eskom KwaZamokuhle AQMS. These concentrations increase with increasing temperature can be attributed to dispersing plumes from tall stacks that are brought down to ground level under unstable atmospheric conditions when thermal turbulence is increased. The bivariate polar plot (Figure 49) also indicates an area of high concentration to the north-west that occur at higher temperatures (10 to 20°C), possibly corresponding to the activities of the power stations. The area of high concentration in the south-easterly direction at temperatures from 10 to 20°C could correspond to vehicle emissions.

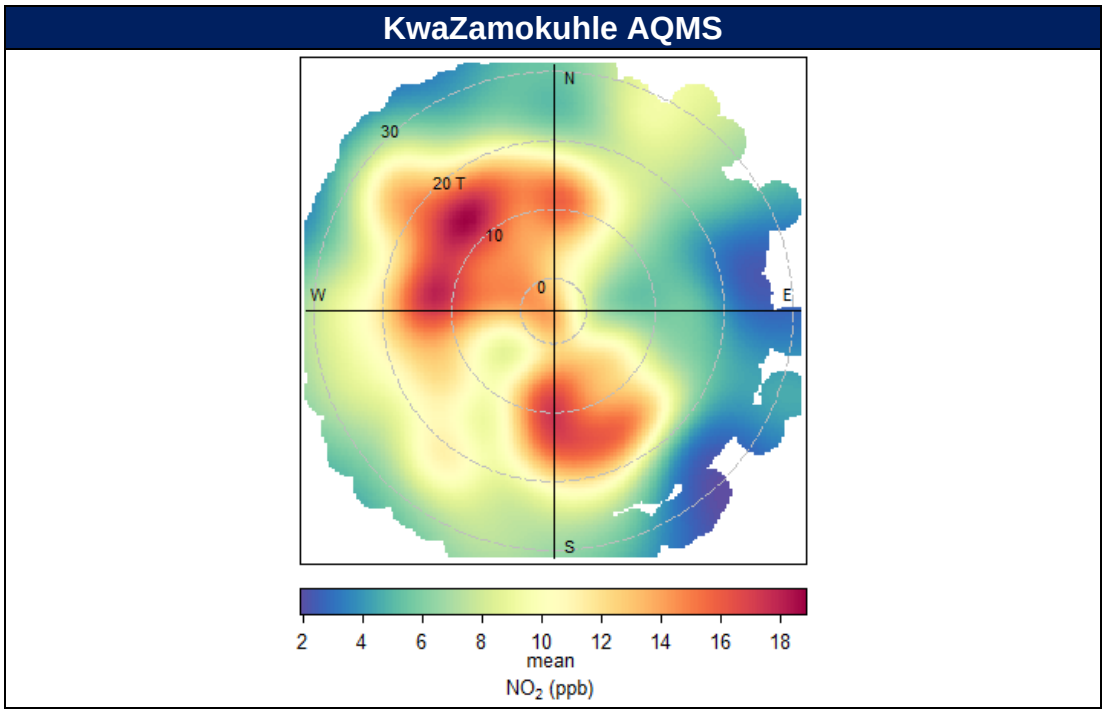

Figure 49: Polar plot of hourly mean NO_2 concentration at the Eskom KwaZamokuhle AQMS for the sampling period.

5. CONCLUSIONS

The daily NAAQS for particulate matter was surpassed at all five residential sampling sites in Kwazamokuhle. The increased levels of particulate matter were most prevalent during the colder winter months, attributed to residential fuel burning. This sampling campaign coincided with the implementation of the Eskom AQO Project intervention in Kwazamokuhle. Following the complete rollout of Eskom AQO Project interventions, a repeat of this monitoring campaign is planned. Furthermore, various scientific studies, including source apportionment, indoor air quality monitoring, and dispersion modeling, will be employed to evaluate the air quality impact after the widespread implementation of Eskom AQO Project interventions.

An evaluation of the Eskom KwaZamokuhle AQMS revealed only one instance of exceeding the hourly SO_2 NAAQS. There were no recorded breaches of the daily SO_2 or hourly NO_2 limits. The SO_2 concentrations were typically linked to residential activities in the afternoon, while the analysis suggested that the variability in NO_2 concentration was connected to vehicle emissions.

This survey campaign clearly indicates that residential fuel burning poses a significant health risk to the Kwazamokuhle community, underscoring the importance of supporting the implementation of Eskom’s PMV air quality offset intervention project in Kwazamokuhle.

6. ACKNOWLEDGEMENTS

Air Resource Management would like to thank the following individuals for their assistance in this study:

- Mr Abel Moatshe and Ms Bontle Moiloa for timeously providing the team with the ambient air quality monitoring data for the Eskom KwaZamkouhle station;
- Mr Motshewa Matimolane and Mr Bryan McCourt for their technical comments and support.

7. REFERENCES

1. S. Munir, T. M. Habeebullah, A. M. F. Mohammed, E. A. Morsy, M. Rehan, and K. Ali, “Analysing $PM_{2.5}$ and its association with PM_{10} and meteorology in the arid climate of Makkah, Saudi Arabia,” Aerosol and Air Quality Research, vol. 17, no. 2, pp. 453–464, 2017.
2. J. Hu, Y. Wang, Q. Ying, and H. Zhang,2014. “Spatial and temporal variability of $PM_{2.5}$ and PM_{10} over the north China plain and the Yangtze River Delta, China,” Atmospheric Environment, vol. 95, pp. 598–609, 2014.
3. Doucet, P., Sloep, P.B. 1992. “Mathematical Modeling in the Life Sciences”, King’s College, London,1992
4. Tiwary, A., Colls, J. “Air Pollution: Measurement, Modeling, and Mitigation”, 3rd Edition, Routledge,New York, 2010
5. Carslaw D.C., Ropkins K. 2012. “Openair – an r package for air quality data analysis”. Environmental Modelling and Software, pp27–28: pp52–61
6. Appel, K.W., Gilliam, R.C., Davis, N., Zubrow, A., and Howard, S.C., 2011. “Overview of the atmospheric model evaluation tool (amet) v1.1 for evaluating meteorological and air quality models”. Environmental Modelling and Software ,Vol 26 (4), pg434-443. http://www.sciencedirect.com/science/article/pii/S1364815210002653
7. Carslaw, D. “The Openair Manual Open-Source Tools for Analysing Air Pollution Data”, King’s College, London, 2015.
8. Czernecki B., Pólrolniczak M., Kkolendowicz L., Marosz M., Kendzierski S., Pilguj N. 2016. “Influence of the Atmospheric Conditions on PM_{10} Concentrations in Poznan, Poland”. Journal of Atmospheric Chemistry,vol 74(1),pp. 1-25. View at: https://www.researchgate.net/publication/308477377_Influence_of_the_atmospheric_conditions_on_PM_{10}_concentrations_in_Poznan_Poland

9. Crilley L.R., Lucarelli F., Bloss W.J., Harrison R.M., Beddows D.C., Calzolai G., Navab S., Vallid G., Bernardonid V., Vecchi R. 2017. “Source apportionment of fine and coarse particles at a roadside and urban background site in London during the 2012 summer ClearfLo campaign”. Environmental Pollution 220: pp766–778
10. Pattinson W., Kingham S., Longley I., Salmond J. 2016. “Potential Pollution Exposure Reductions from Small-Distance Bicycle Lane Separations”. Journal of Transport & Health,Vol 4,pp40-52. View at: https://www.sciencedirect.com/science/article/abs/pii/S2214140516303504
11. Salvador P., Alonso-Pérez S., Pey J., Artíñano B., Debustos J.J., Alastuey A., Querol X. 2014. “African dust outbreaks over the western Mediterranean Basin: 11-year characterization of atmospheric circulation patterns and dust source areas”. Atmospheric Chemistry and Physics Vol 14(13): pp6759–6775. View at: https://www.researchgate.net/publication/263036412_African_dust_outbreaks_over_the_western_Mediterranean_Basin_11-Year_characterization_of_atmospheric_circulation_patterns_and_dust_source_areas
12. Schweizer D.,and Cisneros R. 2014. “Wildland Fire Management and Air Quality in the Southern Sierra Nevada: Using the Lion Fire as a case study with a multi-year perspective on $PM_{2.5}$ impacts and fire policy”. Journal of Environmental Management Vol 144: pp 265–278. View at: https://www.sciencedirect.com/science/article/pii/S0301479714003089?via%3Dihub
13. Crilley L.R., Bloss W.J., Yin J., Beddows D.C., Harrison R.M., Allan J.D., Young D.E., Flynn M., Williams P., Zotter P., Prevot A.S.H., Heal M.R., Barlow J.F.,Halios C.H., Lee J.D., Szidat S., Mohr C., Prevot A.S. 2015. “Sources and contributions of wood smoke during winter in London: Assessing local and regional influences”.

Atmospheric Chemistry and Physics Vol 15(6): pp 3149–3171. View at: https://acp.copernicus.org/articles/15/3149/2015/

14. Jang E., Do W., Park,G., Kim M., Yoo E. 2016. “Spatial and temporal variation of urban air pollutants and their concentrations in relation to meteorological conditions at four sites in Busan, South Korea”. Atmospheric Pollution Research Vol 8(1): pp 89–100. View at: https://www.sciencedirect.com/science/article/abs/pii/S1309104216301192?via%3Dihub
15. Szulecka,A., Oleniacz R , and Rzeszutek,M. 2017. “Functionality of Openair Package in Air Pollution Assessment and Modeling — A Case Study of Krakow”. Environmental Protection and Natural Resources,Vol 28(2):pp 22-27. View at: https://content.sciendo.com/view/journals/oszn/28/2/article-p22.xml?language=en&tab_body=abstract
16. Malby, A.R., Whyatt, J.D., and Timmis, R.J. 2013. “Conditional Extraction of Air-Pollutant Source Signals from air-quality monitoring”. Atmospheric Environment, Vol 74(2013):pp 112-122
17. Carslaw, D.C.,and Carslaw, N., 2007. “Detecting and characterising small changes in ur-ban nitrogen dioxide concentrations”. Atmospheric Environment Vol 41(22): pp 4723-4733.View at: http://dx.doi.org/10.1016/j.atmosenv.2007.03.034
18. Malby, A.R., Timmis, R.J., Whyatt, J.D., 2008. “Combining modelling and monitoring to Estimate Fugitive Releases from a Heavily-Industrialised Site”. Proceedings from the 12th Conference on Harmonisation within Atmospheric Dispersion Modelling for Regulatory Purposes (HARMO 12), Cavtat, Croatia,October 6-9, 2008, pp. 939-943. View at: http://www.harmo.org/Conferences/ Cavtat/12harmo.asp
19. Shu,M., Dang,D., Nguyen,T., Hsu,B., and Pham,K. 2017. “The application of bivariate polar plots and k-means clustering to analysis air pollution in Taoyuan,

Taiwan". International Journal of Advance Engineering and Research Development, Vol 4(4),pp 553-557

20. Carslaw, D.C., Beevers, S.D., Ropkins, K., Bell, M.C., 2006. "Detecting and quantifying aircraft and other on-airport contributions to ambient nitrogen oxides in the vicinity of a large international airport". Atmospheric Environment 40 (28),pp 5424-5434. View at: https://www.sciencedirect.com/science/article/abs/pii/S1352231006004250?via%3Dihub
21. Westmoreland, E.J., Carslaw, N., Carslaw, D.C., Gillah, A., and Bates, E., 2007. "Analysis of air quality within a street canyon using statistical and dispersion modelling techniques". Atmospheric Environment, Vol 41(39), pp 9195-9205. View at: https://doi.org/10.1016/j.atmosenv.2007.07.057
22. Carslaw D.C., and Beevers S.D. 2013. "Characterising and understanding emission sources using bivariate polar plots and k-means clustering". Environmental Modelling and Software, Vol 40: pp 325–329. View at: https://doi.org/10.1016/j.envsoft.2012.09.005
23. Jones, A.M., Harrison, R.M., Baker, J., 2010. "The wind speed dependence of the concentrations of airborne particulate matter and nox". Atmospheric Environment Vol 44(13), pp 1682-1690. View at:http://www.sciencedirect.com/science/article/B6VH3-4Y7P72C-2/2/f6c65e5f49ac3e9862d4c1803d4735c0.
24. Tellaetxe, I.U., and Carslaw, D.C. "Conditional bivariate probability function for source identification",Environmental Modelling & Software,Vol 59,pp 1-9. View at: https://www.sciencedirect.com/science/article/pii/S1364815214001339?via%3Dihub
25. Thangprasert, N.,and Suwanarat,S. 2017. "The Relationships between Wind Speed and Temperature Time Series in Bangkok, Thailand. Journal of Physics:

Conference Series, 901 (2017) 01204. View at: https://iopscience.iop.org/article/10.1088/1742-6596/901/1/012043

26. Grundstrom, M., Tang, L., Hallquist, M., Nguyen, H., Chen, D., and Pleijel,H. “Influence of atmospheric circulation patterns on urban air quality during the winter” Atmospheric Pollution Research,Vol 6(2), pp 278-285. View at: https://doi.org/10.5094/APR.2015.032.
27. Garstang, M., Tyson, P.D., Swap, R., Edwards, M., Kållberg, P. and Lindesay, J.A. (1996). Horizontal and vertical transport of air over Southern Africa. Journal of Geophysical Research, 101 (D19), 23721-23736.
28. Swap, R., Garstang, M., Macko, S.A., Tyson, P.D., Maenhaut, W., Artaxo, P., Kallberg, P. and Talbot, R. (1996). The long-range transport of southern African aerosols to the tropical south Atlantic. Journal of Geophysical Research, 101 (D19), 23777-23791.
29. Held, G., Gore, B.J., Surridge, A.D., Tosen, G.R. and Walmsley, R.D. (eds) (1996), Air Pollution and its Impacts on the South African Highveld, Environmental Scientific Association, Cleveland, 144 pp.
30. DEFF (2010), Air Quality Baseline Assessment for the Highveld Priority Area
31. Merrill, J.T., Bleck, R. and Boudra, D.B. (1986). Techniques of Lagrangian trajectory analysis in isentropic coordinates. Monthly Weather Review, 114, 571-581.
32. Lacaux J.P (2003), IGACtivities Newsletter, issue no.27, January 2003, (http://www.igac.noaa.gov/newsletter/igac27/Jan_2200_IGAC_27.pdf)
33. Martins J.J, Dhammapala R.S, Lachmann G, Galy-Lacaux C and Pienaar J.J., (2007): ‘Long-term measurements of sulphur dioxide, nitrogen dioxide, ammonia, nitric acid and ozone in southern Africa using passive samplers”, South African Journal of Science, 103, 1-7

34. Mphepya J.N. 2004, 'Precipitation Chemistry in Semi-Arid Areas of Southern Africa: A Case Study of a Rural and an Industrial Site', Journal of Atmospheric Chemistry 47: 1–24.
35. Van Zyl, P.G., Conradie, E.H., Pienaar, J.J., Beukes, J.P., Galy-Lacaux, C., Swartz, J., Liousse, C., and Mkhatshwa, G.V., An assessment of precipitation chemistry at the South African DEBITS sites, 13th Quadrennial Symposium of the International Commission on Atmospheric Chemistry and Global Pollution, (iCACGP) 13th Science Conference of the International Global Atmospheric Chemistry Project, (IGAC), Natal Convention Center (NCC), Natal, Brazil 22-26th September 2016
36. Van Zyl, P.G., Beukes, J.P.;Conradie, E.H.; Pienaar, J.J.; Mkhatshwa, G.; Fourie, G.D. and Galy-Lacaux, C., Deposition measurements in southern Africa, Workshop on Atmospheric Depostion Processes, The Abdus Salam International Centre for Theoretical Physics, Trieste, Italy, 21-25 May 2012.
37. P. Maritz, J.P. Beukes, P.G. van Zyl, E.H. Conradie, A.D. Venter, J.J. Pienaar, C. Liousse, C. Galy-Lacaux, Spatial and temporal assessment of atmospheric organic and black carbon concentrations at South African DEBITS sites, 16th International Union of Air Pollution Prevention Association (IUAPPA) Congress, 29 September – 4 October 2013, International Convention Centre, Cape Town, South Africa.

DISCLAIMER

Air Resource Management (Pty) Ltd has prepared this report based on an agreed scope of work and acts in all professional matters as an advisor to the Client and exercises all reasonable skill and care in the provision of its professional services in a manner consistent with the level of care and expertise exercised by air quality management professionals.

Reports are commissioned by and prepared for the exclusive use of the Client. They are subject to and issued in accordance with the agreement between the Client and Air Resource Management (Pty) Ltd. Air Resource Management (Pty) Ltd is not responsible and will not be liable to any other person or organisation for or in relation to any matter dealt within this Report, or for any loss or damage suffered by any other person or organisation arising from matters dealt with or conclusions expressed in this report (including without limitation matters arising from any negligent act or omission of Air Resource Management (Pty) Ltd or for any loss or damage suffered by any other party relying upon the matters dealt with or conclusions expressed in this Report). Other parties should not rely upon the report or the accuracy or completeness of any conclusions and should make their own inquiries and obtain independent advice in relation to such matters.

Except where expressly stated, Air Resource Management (Pty) Ltd has not verified the validity, accuracy or comprehensiveness of any information supplied to Air Resource Management (Pty) Ltd for its reports.

Reports prepared by Air Resource Management (Pty) Ltd cannot be copied or reproduced in whole or part for any purpose without the prior written agreement of Air Resource Management (Pty) Ltd.

Where site inspections, testing or fieldwork have taken place, the report is based on the information made available by the client or their nominees during the visit, visual observations and any subsequent discussions with regulatory authorities. The validity and comprehensiveness of supplied information has not been independently verified and, for

the purposes of this report, it is assumed that the information provided to Air Resource Management (Pty) Ltd is both complete and accurate. It is further assumed that normal activities were being undertaken at the site on the day of the site visit(s), unless explicitly stated otherwise.

COPYRIGHT